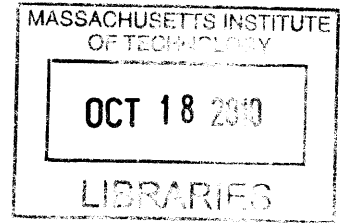# Modeling and Vehicle Performance Analysis of Earth and Lunar Hoppers

by

Akil J. Middleton

B.S. Aeronautics and Astronautics
Massachusetts Institute of Technology, 2008

Submitted to the Department of Aeronautics and Astronautics
in Partial Fulfillment of the Requirements for the Degree of

Master of Science in Aeronautics and Astronautics

at the

MASSACHUSETTS INSTITUTE OF TECHNOLOGY

September 2010

Signature of Author:...
Department of Aeronautics and Astronautics
August 19, 2010

Certified by:......
Jeffrey Hoffman
Professor of Aeronautics and Astronautics
Thesis Supervisor

Certified by:......
Stephen C. Paschall II
Senior Member of the Technical Staff, Draper Laboratory
Thesis Supervisor

Accepted by:......
Eytan H. Modiano
Associate Professor of Aeronautics and Astronautics
Chair, Committee on Graduate Students

Modeling and Vehicle Performance Analysis of Earth and Lunar Hoppers

by

Akil J. Middleton

Submitted to the Department of Aeronautics and Astronautics
on August 19, 2010, in Partial Fulfillment of the
Requirements for the Degree of
Master of Science in Aeronautics and Astronautics

Abstract

Planetary hoppers–vehicles which travel over the surface as opposed to on it–offer significant advantages over existing rovers. Above all, they are able to travel quickly and can overcome terrain obstacles such as boulders and craters. The Next Giant Leap team in the Google Lunar X- PRIZE competition plans on utilizing hopper technology for its design, but they have little from which to work. In fact, although hopper-like vehicles have been created and flown, none have been used to serve specifically as tools for planetary exploration. Thus it is clear that prototyping and modeling will have to be done in order to gauge the feasibility of such a system. To support this effort, this thesis provides a look into the performance of hopper technologies through modeling and simulation. It begins by using the Hop Tradespace Tool to examine the two fundamental hop trajectories, determining that although there is a fuel savings with the ballistic hop, the hover hop is more desireable for testing. This result is then applied to a preliminary mission analysis for the TALARIS prototype vehicle. Finally, the Earth TALARIS and its lunar version are modeled in 3-DOF simulation and it is discovered that, even with error and uncertainty, TALARIS closely emulates what would be expected to be seen on the Moon.

Thesis Supervisor: Jeffrey Hoffman
Title: Professor of Aeronautics and Astronautics

Thesis Supervisor: Stephen C. Paschall II
Title: Senior Member of the Technical Staff, Draper Laboratory

Acknowledgments

This thesis journey would not have been possible without the help of many different people filling a variety of roles. At the top of this list are my two advisors: Professor Jeff Hoffman and Steve Paschall. I have to thank Prof. Hoffman for providing a sense of symmetry to my academic research career: he first helped me find a UROP as a freshman, and now he has guided me through the greater part of my graduate years. As for Steve, my Draper advisor: the process took a little longer than expected, but it was absolutely worth it. I learned more from you than can be reflected in this thesis. Thanks for your time, patience, and for preparing me to join the real world of engineering.

Other Draper employees who assisted me and helped me feel comfortable over the past two years deserve a mention too. There's Bobby Cohanim, who initially introduced me to the hopper project and was like an advisor in that area. And then we have Mike Johnson, who taught me what control engineers do, and Linda Fuhrman, who assisted me from the moment I was accepted as a Draper Fellow and didn't stop until my thesis was turned in. Thanks, all, for your support (although I know it was sometimes a struggle with me being a Yankees fan).

Also from the academic side, I must thank the many members of the TALARIS team. I apologize for spending more time at Draper than on campus, but I hope this thesis proves that I really *was* getting work done! I look forward to joining you again in the fall.

A thesis is all about learning and research, but without a life outside of that you're bound to go crazy. Thanks especially to my good friends Holly and Amanda for also deciding to continue the Course XVI experience after undergrad. And thanks to those who we picked up along the way: Aaron, Brett, and my future roommates Ben and Torin. Best of luck to those of you who are going for that PhD!

And certainly, TKP to my brothers of the Rho Alpha Chapter of the Zeta Psi Fraternity for allowing me to stay in the house for two additional years. It has been a blast, but now this "old guy" will finally get out of your hair.

And last but definitely not least: I'd like to thank my mom, dad, and sister, as well as my grandma and aunt in Indiana, for always believing in my potential.

_____ 8/19/2010

Akil J. Middleton   Date

Contents

THIS PAGE INTENTIONALLY LEFT BLANK

List of Figures

THIS PAGE INTENTIONALLY LEFT BLANK

List of Tables

THIS PAGE INTENTIONALLY LEFT BLANK

Chapter 1

Introduction

Since their initial use in the 1970's, ground-based rovers have been the primary mode of robotic planetary surface exploration. Nevertheless, they still have their shortcomings. With respect to landing operations, rovers require a lander from which they can be initially deployed. This both adds to the mass of the mission and leads to added complexity in removing the vehicle upon reaching the ground. From a functional standpoint, traditional rovers are limited in the types of terrain over which they can travel. They are well-suited for relatively flat ground, but are unable to climb steep cliffs, pass over crevices, and extract themselves from ground hazards. Current rover technology may limit mission capabilities if a goal is to explore more dangerous and diverse planets, moons, and asteroids.

It is for this reason that the concept of surface hoppers is being investigated. Unlike rovers which travel while in contact with the ground, a hopper reuses its landing propulsion system to lift off and travel to its destination above the terrain. By reusing the descent engines, mass is conserved since a separate lander is no longer required. Also, its method of movement, the "hop", allows the vehicle to pass over terrain obstacles that would limit the progress of rovers. Certainly, hoppers represent a technology which could provide significant utility for planetary exploration.

Although the theory of hoppers sounds promising, little research has been done on their actual capabilities. Hopper-like vehicles, such as USC's LEAPFROG and entries in the Northrup Grumman Lunar Lander Challenge, have been constructed

and flown, but their goals have been mainly to serve as testbeds for lunar hardware as opposed to being prototypes of actual vehicles. The Next Giant Leap team's entry into the Google Lunar X-PRIZE will be the first hopper designed for surface exploration, but this use of the technology has been previously untested. Thus it is clear that prototyping, modeling, and analysis will have to be done in order to fully characterize the pros and cons of a hopper system.

1.1 Motivation

1.1.1 Google Lunar X-PRIZE

The Google Lunar X-PRIZE is an international competition to land a vehicle on the surface of the Moon, traverse a given distance, and send data back to Earth. Twenty privately-funded teams are currently registered. To win the grand prize, a team must have its vehicle travel at least 500 meters and send back a predefined data package of photograph and video called a "Mooncast." There is also a second prize to encourage the continuation of the competition. Bonuses are available as well: extra prize money will be awarded for tasks such as traveling longer distances, taking pictures of Apollo artifacts, and discovering water and ice. The competition is slated to end on December 21st, 2014 [2].

Next Giant Leap is one of the many teams that has entered into the X-PRIZE competition. Its technical members are the Sierra Nevada Corporation, the Massachusetts Institute of Technology's (MIT) Space Systems Lab, the Charles Stark Draper Laboratory, and Aurora Flight Sciences. Although the team is focused on winning the X-PRIZE, its long-term goal is "*[T]o provide affordable commercial services in support of lunar and other solar system exploration leading to a sustainable expansion of human presence in our solar system*"[2]. In other words, it is looking to establish a new vehicle for space exploration. To achieve these ends, Next Giant Leap has decided to steer away from the traditional rover concept and push forward with a hopper design, hereby referred to as the Next Giant Leap vehicle (NGL).
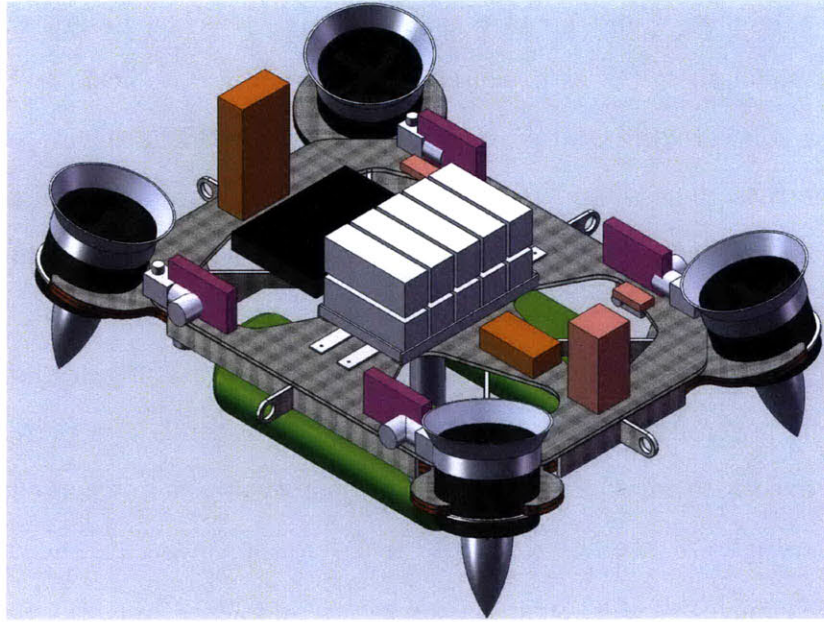
Figure 1-1: CAD model of TALARIS-2

Because hoppers are a novel concept, there is a need to develop a prototype to test its capabilities before the lunar mission. This task became the responsibilty of MIT and Draper Laboratory in the form of TALARIS.

1.1.2 TALARIS

TALARIS, or the *Terrestrial Artificial Lunar And Reduced gravIty Simulator*, is a lunar hopper prototype being developed at MIT to support the Next Giant Leap project. At the present time, the vehicle has a roughly 0.5 meter by 0.5 meter frame which holds its batteries, electronics, navigation equipment, and four electric ducted fan engines (EDFs). Upon completion, TALARIS will have a slightly larger body and will see the addition of a fully functional cold gas thruster system (CGS). These eight fixed thrusters will serve as the vehicle's primary propulsion system. An image of the final state of TALARIS is seen in figure 1-1.

The plan is for TALARIS to serve primarily as a testbed for lunar hopper guidance, navigation, and control algorithms. For the system to properly test the software, the vehicle must work in a simulated lunar environment. Creating this is the job of the EDFs: the fans have the responsibility of carrying 5/6 of the vehicle's weight, leaving

19

an effective weight as would be seen on the Moon. Such a design will allow the software to control the CGS as it would the lunar propulsion system. There is also going to be a software "translator" between the TALARIS hardware and the lunar software. The reasoning behind this is twofold: it will prevent the lunar algorithms from being exposed to Earth-only disturbances, and also will convert lunar actuator commands into a form which will work on the test vehicle.

Assuming TALARIS functions as expected, there are still questions to be answered. Is the hover-style of hop, where the vehicle ascends and performs a fixed-attitude and fixed-altitude traverse, the best trajectory option in terms of performance metrics such as delta-V and hop duration? Furthermore, what are the capabilities of TALARIS and will it be able to emulate what is expected to be seen on the Moon? These questions guided the studies described in this thesis.

1.2   Previous Work

Since a hopper is a proposed method of planetary exploration, it is helpful to look at the history of vehicles designed for this purpose. This section begins with a brief overview of rover technology and will then discuss recent hopper-like projects.

1.2.1   History of Planetary Rovers

1.2.1.1   The Lunokhod Program

The Soviet Lunokhod-1 was the first unmanned vehicle to land softly on another planetary body. Launched in the Luna 17 vehicle on November 11, 1970, the Lunokhod-1 was deployed in the Moon's Sea of Rains five days later. The rover was 756 kilograms, 2.2 meters in both length and width, and reportedly reached a top speed of 0.27 m/s [11]. The mission was planned to have a duration of three lunar days but actually lasted for eleven; operations ceased on October 4th, 1971 [9]. This roughly eleven-month lifespan would only be eclipsed by the Mars Exploration Rovers over 30 years later.

Lunokhod-1 was unmanned but it was still remote controlled; human operators sent commands and interpreted data back on Earth. There were two ground crew teams which rotated ten to twenty times a lunar day. Each consisted of five engineers with various jobs: the crew chief, who oversaw all operations; the driver, who was responsible for moving the rover; the navigator, who interpreted state data and planned the vehicle's course; the antenna operator, who controlled the antenna; and the engineer, who oversaw a subteam responsible for analyzing telemetry and the rover's condition [11]. Operating the Lunokhod-1 was a complex task of synthesizing data from various crew members while compensating for a 5-second delay between the transmission of a command and its execution on the Moon.

The Soviet rover was equipped with "*[A] cone-shaped antenna, a highly directional helical antenna, [and]* four television cameras" [9]. These were for transmitting image and state data and receiving commands from the ground. For science, it had "*[S]*pecial extendable devices to impact the lunar soil for soil density and mechanical property tests *[...]*, *[a]*n x-ray spectrometer, an x-ray telescope, cosmic-ray detectors, and a laser device" [9]. The vehicle itself was powered by solar and chemical batteries. Its only two purely autonomous functions were soil testing operations and a power-down in the instance where the vehicle moved outside its allowed range of motion [11]. At the end of its eleven-month mission, Lunokhod-1 traveled about 10.5 kilometers, transmitting over 20,000 pictures and conducting more than 500 tests on the lunar soil.

Lunokhod-2 was launched aboard the Luna 21 vehicle on January 8th, 1973 and was deployed on the Moon on January 15th. The second model was more massive than its predecessor at 840 kilograms, but it was more compact at 1.70 meters long and 1.60 meters wide [10]. As with Lunokhod-1, Lunokhod-2 was remotely operated by a five-man crew on Earth. It also performed similar science experiments.

The second Lunokhod mission improved over the first in two ways. One, the navigation cameras were upgraded and sent images every three seconds; this aided the accuracy of the driver in the ground station. Two, the ground crew team itself was more experienced [6]. These two factors led to an improved average performance for

the vehicle: Lunokhod-2 traveled about 37 kilometers in four months, compared to the 10.5 kilometers in eleven months of Lunokhod-1 [10]. Nevertheless, large mechanical systems would be its downfall. A navigation miscalculation resulted in the rover running into the side of a crater, causing lunar soil to fall onto the solar cells on its lid. When lunar nightfall arrived and the lid had to be closed, the soil fell onto the rover's radiator, preventing it from properly cooling the rover. The Lunokhod would overheat come morning and vehicle operations would cease [6].

1.2.1.2 American Mars Rovers

Although the United States featured manned rovers in all Apollo missions from 15 and beyond, Sojourner was the country's first semi-autonomous rover and was the first in the world to be sent to another planet. Sojourner, the rover component of the Mars Pathfinder Mission, was deployed from the Pathfinder Lander in July of 1997. This "microrover" had a significant size reduction from the earlier Soviet models: it was 11.5 kilograms, 0.28 meters in height, 0.630 meters long, and 0.480 meters wide. Its maximum speed was around 0.01 m/s [1].

The primary goal of the rover mission was to show that small rovers could operate on a foreign planet. This was accomplished; Sojourner outlived its design life by twelve times the expected duration, lasting just over 83 days instead of the planned seven. During this period it executed a number of tests, including but not limited to chemical analyses of Martian rocks and soil, logging of vehicle performance, imaging and telemetry tests, and gathering of atmospheric data. It also transmitted 550 images back to the ground [4].

One key difference in operation between Sojourner and the Lunokhods was its method of control. Due to the 11-minute travel time for a command to reach Mars, it was not feasible to have drivers and navigators fully operate the vehicle from Earth. For this reason Sojourner had to be mostly autonomous. The role of ground crew was to use terrain images, received at the end of each day, to understand the layout of the rover's location. The operator would then use the images as a mean to establish a set of waypoints for the rover's next trajectory. These, along with navigation correc-

tions, were then transferred to the vehicle. The rover would then use its own lasers and camera to reach the desired waypoints while using onboard hazard avoidance procedures [1].

The most recent rover mission also involves Mars. The Mars Exploration Rover (MER) mission was launched in 2002 and is still in progress today. The two twin vehicles, Spirit and Opportunity, were released on opposite sides of the planet in a primary effort to search for signs of previous water on the planet. At 2.3 meters wide by 1.6 meters long and 1.5 meters tall each, the two rovers have traveled for a combined 4300 days for over 27.0 kilometers while performing numerous planetary and atmospheric experiments [8, 13].

The MER produced robots with the highest level of autonomy seen in rovers to date. They not only utilize various hazard avoidance technologies, but they are also equipped with tools to correct for heading changes and able to select best paths on their own. Furthermore, the ability to update the vehicle software from the ground keeps the door open for improvements [12]. Rover technology has certainly matured from the completely human-controlled Soviet models.

Nevertheless, the MER vehicles are still hindered by design limitations. During April of 2009, the Spirit vehicle broke through a thin layer of ground and became embedded in the soil underneath. The engineers tried various extraction methods for ten months to no avail. Unable to remove the rover from this hazard, the operators have decided to designate the vehicle as a stationary science platform [13].

1.2.1.3 Rovers in Summary

Despite design maturation since the days of Lunokhod, there remain significant short-comings to rover performance. First, they are slow. Even the MER vehicles can only obtain a top speed of 0.05 m/s, which doesn't include the time-averaged velocity as they stop and check for hazards. This is not acceptable for situations in which a quick traversal across the surface, or travel over long distances, is required. Secondly, solar powered propulsion has a virtually unlimited power source, but it limits when the vehicle can be fully operational. In contrast, a chemical propulsion system, while

also having its own limitations, could function at any time during the day or night. And three, by being ground-based, exploration is limited by steep cliffs, boulders, and sand traps. These three factors restrict the operating ranges of rovers, and overcoming them is where hoppers can prove useful.

1.2.2 Existing Hopper Projects

In 2007, the University of Southern California's Information Sciences Institute and Astronautics and Space Technology Division created LEAPFROG "as a solution to the challenges associated with the development and testing of lunar landing technologies" [7]. Specifically, its goal was to be similar to the NASA Lunar Landing Research Vehicle (LLRV) and serve as a low-cost reusable testbed for lunar technology development. The student run project was required to ascend, hold an altitude, and translate while remaining stable. It was also designed to be completely autonomous, with only start and stop commands sent from the ground station. This is essentially the "hover hop" that NGL and TALARIS will be performing.

The Northrup Grumman Lunar Lander Challenge has been held from 2006 through 2009 in an effort to accelerate the development of commercial lunar landing technology [3]. The competition consists of two parts: the first requires a designed vehicle to launch to an altitude of 50 meters, maintain a hover, traverse and land on a pad 50 meters away, and then follow the trajectory in reverse. The second part is the same as the first with the additional requirements that the vehicle hover for twice as long, and that the landing pad is now a rocky simulated lunar surface. Like with LEAPFROG, this is essentially a hover hop. Yet unlike NGL and TALARIS, the winning designs in the Lunar Lander Challenge feature a single gimbaled main engine for vertical thrust.

The key point about these existing "hoppers" is that establishing a hop as a method of surface mobility was not the primary goal. LEAPFROG is a testbed for lunar landing hardware, while one of the purposes of the Lunar Lander Challenge mission is to "[represent] *the technical challenges involved in operating a reusable vehicle that could land on the moon*" [5]. Although they show that such a maneuver is possible, they say nothing about its feasibility as a planetary surface mobility technique or the

difficulties introduced by using smaller, fixed thrusters for vehicle translation.

1.3 Thesis Overview

The goal of this thesis is to provide a look into the performance of hopper technologies through modeling and simulation. Chapter 2 will examine the two fundamental hop trajectories, the ballistic and hover hop, in order to determine which is most desireable. Chapter 3 will use this conclusion and apply it to a preliminary mission analysis for the TALARIS prototype vehicle. Chapter 4 will build upon the analysis presented in the previous chapter by modeling the TALARIS and NGL vehicles in simulation in order to determine to what extent the Earth vehicles can emulate their lunar counterparts. Finally, Chapter 5 will present a summary of findings, the limitations present in this study, and steps for progressing further with this line of research.

THIS PAGE INTENTIONALLY LEFT BLANK

Chapter 2

Hop Performance Analysis

TALARIS and NGL are slated to perform a "hover hop" due to the maneuver's apparent simplicity. Nevertheless, it is unclear if this qualitative advantage outweighs any of its potential quantitative shortcomings. For example, are there other hop methods that may be more complex but consume significantly less fuel? The chapter describes the first-order performance analysis carried out to investigate the pros and cons of the hover and ballistic hop maneuvers while using the Moon as the setting.

2.1 Problem Formulation

2.1.1 Fundamental Hop Trajectories

There are two fundamental types of hop: the ballistic and hover. Their shapes are seen in figure 2-1. A ballistic hop begins with the vehicle lifting off by performing a delta-V maneuver at a nonzero angle relative to the surface. This places it into a ballistic coast. As the vehicle approaches the surface for landing, it performs a brake to reduce its velocity for a soft touchdown. This hop method only requires engine thrust at launch and landing.

With a ballistic hop the vehicle is able to reach high altitudes due to its arc-shaped trajectory. During the powered launch and landing phases, its attitude is generally constrained in order to perform the delta-V maneuver in the appropriate direction.
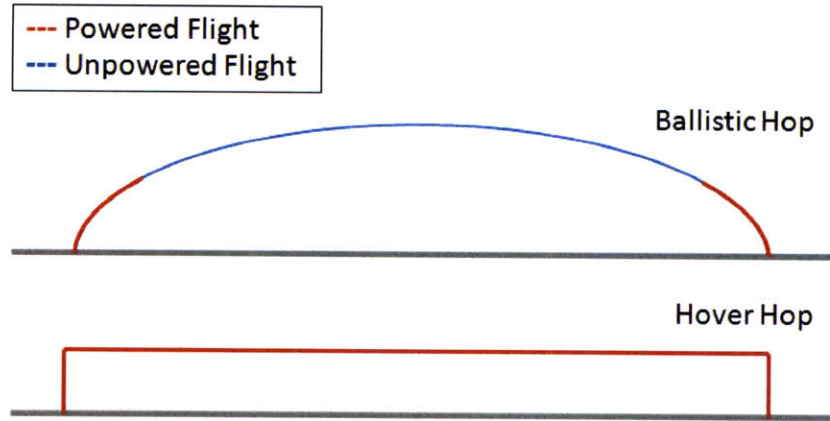
Figure 2-1: The Fundamental Hop Trajectories. The red represents when the engines are on, whereas the blue is when the engines are off.

Between these two powered phases, however, there are no restrictions on vehicle orientation. This unconstrained attitude could be beneficial for reorienting itself to collect terrain data from onboard instruments or providing a steady communication link. One downside of the ballistic hop is that the powered maneuvers are relatively brief, so accurate execution is necessary for precise targeting.

The hover hop starts with the vehicle ascending to a predetermined hover height above the lunar surface: it accelerates away from the ground, throttles appropriately in order to zero its velocity at the specified height, and then continues to thrust at one lunar-g in order to maintain altitude. Next, the vehicle accelerates downrange to start its traverse. It then turns off its horizontal engines while continuing to coast and provide the one lunar-g acceleration against gravity. When it gets halfway to the desired distance, it will follow these steps in reverse; specifically, it will coast, accelerate uprange to brake and eliminate downrange velocity, and then descend to a soft touchdown. This maneuver was predicted to be more fuel expensive because engines remain on for the entire hop.

A vehicle performing a hover hop maintains a fixed height and has its attitude constrained for the mission. This constrained attitude will likely be steady for the flight, which could also be useful for close inspection of the terrian or for providing a steady communication link. Since the powered maneuver lasts the entire hop, there is the opportunity to make small, gradual trajectory error corrections should they
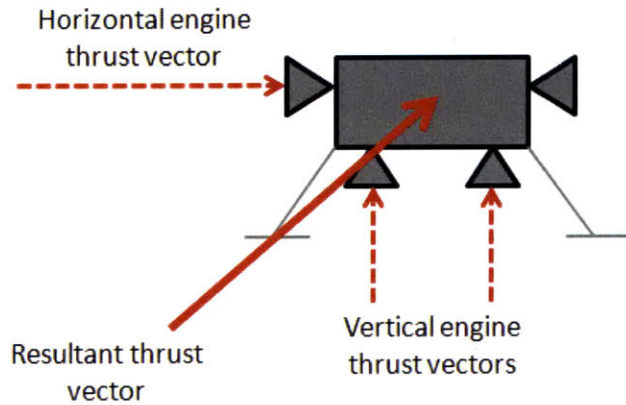
Figure 2-2: Hopper Schematic. The resultant thrust vector shown here would be used for a ballistic hop.

prove necessary[1].

These trajectories are considered fundamental due to the fact that any maneuver in practice will most likely combine ascpects of both. That is, a ballistic hop will require a brief ascent phase to initially get the hopper off the ground, and the hover hop will require less fuel if the vehicle traverses and rises to hover height simultaneously. Thus, by investigating both fundamental hops the bounds on performance can be established.

2.1.2 Vehicle Model

The hopper used in this analysis is similar to the design of TALARIS and NGL. It has two sets of engines: one responsible for vertical thrust and the other for lateral thrust. With the ability to throttle each as necessary, the vehicle can control the direction and magnitude of the resultant thrust vector without needing to reorient itself; this decouples vehicle attitude from vehicle thrust direction. With this configuration, only the translational three degrees of freedom (3-DOF) were needed to analyze the vehicle's performance. The hopper used here has an initial 100 kg wet mass and engines with specific impulses of 300 seconds. A schematic of the vehicle is seen in figure 2-2.

---

[1]The specifics of correcting these errors will not be touched upon in this study.

2.1.3 Assumptions

A number of assumptions were made in order to simplify this analysis. They are:

- The vehicle has perfect state knowledge. There are no trajectory dispersions due to navigation errors.

- The vehicle has perfect state control. Throttle control is perfect and instantaneous and there are no trajectory dispersions due to control errors.

- Similarly, the hopper has ideal actuators and there is an insignificant time delay between the phases of a maneuver.

- All hops are fixed attitude maneuvers. Since there are no trajectory dispersions, there are no attitude dispersions either.

- Due to the previous assumptions, the motion of the vehicle is constrained to a two-dimensional plane.

These assumptions mean that the performance analysis will produce idealized and first-order results. Although some of the simplifications are unrealistic, they still help to establish an upper bound on vehicle performance by showing the best that can be achieved.

2.1.4 Outline of Experimental Approach

A hop is defined by a number of values, e.g. engine thrust and burn time. As such, examining the performance of a hop requires carrying out a parametric analysis across all variables. The end result of this approach is a tradespace from which trends can easily be viewed and compared.

The method used in this study is outlined as follows. First, a set of MATLAB scripts is developed to simulate both a ballistic and hover hop on the Moon. Then a wrapper function is created to run the scripts multiple times while changing hop parameters and storing relevant values. Finally, the data is assembled, reduced, and analyzed. From here conclusions can be made about the performances of each hop.

2.2 Analysis Tool Description

The Hop Tradespace Tool (HTT) is a suite of MATLAB scripts that is able to run hop simulations and generate a tradespace by varying parameters of a hop. It consists of a ballistic tool, a hover tool, and a wrapper. This section will go into the structure and development of the HTT.

2.2.1 General Equations

Before equations can be presented, the coordinate system used by the HTT must be defined. The radial unit vector $\hat{r}$ is equal to the local vertical unit vector $\hat{\mathbf{UP}}$. If the out-of-plane crosstrack vector, $\hat{\mathbf{CT}}$, is defined as $\begin{bmatrix} 0 & 0 & -1 \end{bmatrix}$, the local downrange unit vector is:

$$\hat{\mathbf{DR}} = \hat{\mathbf{CT}} \times \hat{\mathbf{UP}} \tag{2.1}$$

The three vectors $\hat{\mathbf{UP}}$, $\hat{\mathbf{CT}}$, and $\hat{\mathbf{DR}}$ define a right-handed coordinate system. Forward motion will be in the $+\hat{\mathbf{DR}}$ direction, and movement away from the surface will be in the $+\hat{\mathbf{UP}}$ direction. These vectors are recalculated at each simulation timestep.

The general equation of motion is:

$$\ddot{\vec{r}} = \vec{a}_{grav} + \vec{a}_{eng} \tag{2.2}$$

where $\vec{r}$ is the hopper's position measured from the center of the planet, $\vec{a}_{grav}$ is the acceleration due to gravity, and $\vec{a}_{eng}$ is the acceleration from the engines. These accelerations can be broken down as follows:

$$\vec{a}_{grav} = -\frac{\mu}{r^2}\hat{r} \tag{2.3}$$

$$\vec{a}_{eng} = a_{eng}\hat{\imath}_{eng} \tag{2.4}$$

31

with μ defined as the gravitational parameter for the planet, r as the distance between the vehicle and the planet's center, $\hat{r}$ representing the radial unit vector, a_{eng} being the magnitude of the engine acceleration, and the unit vector $\hat{i}_{eng}$ pointing in the direction of the engine acceleration. When divided into components, 3.2 becomes:

$$\vec{a}_{eng} = a_H \hat{\mathbf{DR}} + a_V \hat{\mathbf{UP}} \tag{2.5}$$

Here, a_H and a_V represent the magnitudes of the horizonal and vertical accelerations, respectively [2].

When $\vec{a}_{grav}$ and $\vec{a}_{eng}$ are defined, equation 3.1 can be integrated forward in time. For the HTT, this is done with the use of a Runge-Kutta 4th order integrator.

The change in mass is calculated from:

$$\dot{m} = -\frac{T}{Isp \cdot g_{earth}} \tag{2.6}$$

T is the engine thrust and can also be written as $(a_H + a_V)m$, Isp is the specific impulse of the engines, and g_{earth} is Earth's gravitational acceleration. When this equation is integrated the result is the lost mass. In the HTT this integration is carried out via the Euler method and is performed at every timestep.

Equations 3.1 through 3.8 are used prominently in the HTT to carry out the ballistic and hover hops. This will be described in detail in the next section.

2.2.2 Ballistic Tool

The ballistic tool takes in the following values as inputs:

- Thrust, T (N)

- Takeoff engine burn time, t_{burn} (s)

---

[2] This is an acceptable formulation due to the assumption that the vehicle maintains a fixed attitude, and as such the engines will always point in the horizontal and vertical directions.
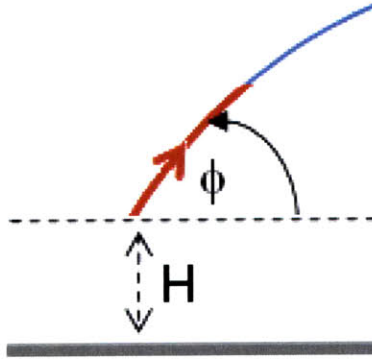
Figure 2-3: Ballistic hop inputs. The arrow represents the thrust, and the red line represents the takeoff engine thrust time.

LUNAR g	1.623 m$/s^2$
LUNAR μ	4.903×10^{12} m^3/s^2
RADIUS OF THE MOON, R	1737.4×10^3 meters
EARTH g	9.81 m$/s^2$
SIMULATION TIMESTEP, dt	0.01 seconds

Table 2.1: HTT parameters for a lunar hop

- Launch angle relative to the local horizontal, ϕ (radians)

- Initial launch height, H (m) [3]

A diagram is seen in figure 2-3. The tool also uses the parameters listed in table 2.1. Using this information, the tool simulates the phases of a ballistic hop. They are the launch, coast, and braking phases.

Launch Phase

The ballistic launch phase runs until the takeoff engine burn time specified by the user is met. The thrust direction $\hat{i}_{eng}$ is obtained from normalizing the vector sum $\tan(\phi) \cdot \hat{\mathbf{UP}} + \hat{\mathbf{DR}}$. The magnitude of the acceleration, a_{eng} is T/m. Multiplying these together results in $\vec{\mathbf{a}}_{eng}$ as seen in equation 3.2 [4]. With this, the state can be propagated forward in time by integrating equation 3.1 across each timestep.

---

[3]This was set to zero for this analysis, but the capability still exists.

[4]The vertical component of the launch acceleration must be greater than 1 lunar-g for the hopper to take off. If this is not the case, the simulation will stop and output an error message.

When the launch phase ends, the vehicle altitude, h, at the time of engine power off is retained. It will be utilized in the braking phase.

Ballistic Phase

The ballistic phase is more straightforward than the launch. Here, the engine acceleration is set to zero. The state is propagated, and the effect is that the vehicle goes into a ballistic coast. Keep in mind that this phase is completely unpowered, and as such, no mass is lost.

Braking Phase

The final phase of the ballistic hop is the braking phase. It is triggered when h, the height reached at the end of the launch, is reached again. The first part of the brake consists of the vehicle slowing down by thrusting in a direction opposite its takeoff thrust vector. In other words, the engine acceleration unit vector $\hat{\imath}_{eng}$ is now obtained from normalizing $\tan(\phi) \cdot \hat{\mathbf{UP}} - \hat{\mathbf{DR}}$. The magnitude of the acceleration remains $a_{eng} = T/m$, resulting in the proper value of $\vec{\mathbf{a}}_{eng}$. This vector is used to propagate position and velocity forward in time.

The second portion of the brake is designed to create a soft touchdown [5]. The goal is to land with a vertical velocity of -2.0 m/s. When this speed is reached by the hopper, three values are calculated:

1. The *fall time* (s), or the time in which it will take the vehicle to hit the ground given its current altitude and the vertical velocity [6]. This is calculated by dividing the current altitude by -2.0 m/s.

2. The *downrange velocity*, v_{DR}. This is the dot product of the velocity vector and $\hat{\mathbf{DR}}$.

3. The horizontal landing acceleration magnitude, a_{land}. This value comes from dividing v_{DR} by the fall time. As a result of its construction, this is the hori-

---

[5]The launch cannot be simply done in reverse. This is because the vehicle has lost mass, and reusing the same thrust as launch would prevent it from landing.

[6]This is constant at -2.0 m/s.

zontal acceleration needed to land with a "small" downrange velocity as to not damage the vehicle.

Using equation 2.5, $a_H = a_{land}$, and $a_V = g_{lunar}$ to maintain the constant vertical velocity. These lead to $\vec{a}_{eng}$, which is the total engine acceleration necessary to perform a soft landing. The state is propagated with this value until the hopper reaches the surface.

2.2.3 Hover Tool

The hover tool takes in the following values as inputs:

- Ascent engine thrust, T_V (N)

- Traverse engine thrust, T_H (N)

- Horizontal thrust time, t_{thrust} (s)

- Hover height, H (m)

- Half of the traverse distance, d_{half} (m)

It also uses the same parameters as the ballistic hop listed in table 2.1. These allow the simulation to complete the three phases of a hover hop. Note that unlike the ballistic hop, the hover maneuver's ascent can be decoupled from the rest of the maneuver. Furthermore, the tool only simulates half of a hover hop. This is primarily to save on processing time, but is acceptable because the second half of the trajectory will be almost identical to the first.

Ascent

The ascent algorithm utilized for the hover tool is an analytic solution to the best-case scenario. In other words, it presents the fuel-optimal maneuver in which the hopper is able to turn off its engines such that it vertically coasts and reaches the desired hover height H with zero velocity [7]. The solution is derived as follows:

---

[7]Although not feasible in the real world, a guidance law could be developed to deliver similar results.
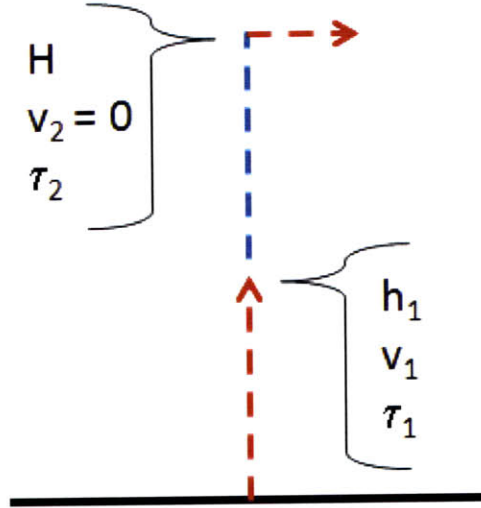
Figure 2-4: Hover hop ascent. Red represents engines on while blue is when the engines are off.

The ascent is divided into a powered and coast section and can be seen in figure 2-4. At the end of the powered lift-off, the hopper's position can be described by the constant acceleration kinematic equation:

$$h_1 = \frac{1}{2}(a_V - g)\tau_1^2 \tag{2.7}$$

where a_V is T_V/m, τ_1 is the time at the power-down, and h_1 is the height reached at this point. Note that h_1 is an unknown and the goal is to solve for τ_1. The kinematic equations for the velocities are:

$$v_1 = (a_V - g)\tau_1 \tag{2.8}$$

$$v_2 = v_1 - g\tau_2 \tag{2.9}$$

where equation 2.8 is the velocity at the end of the lift-off, and equation 2.9 is the velocity when the hopper reaches H. However, at this point v_2 should be equal to zero, which leads to a relationship between v_1 and τ_2. Substituting equation 2.8 into equation 2.9 yields the following:

$$\tau_2 = \frac{(a_V - g)}{g} \tau_1 \tag{2.10}$$

When the vehicle arrives at H at the end of the vertical coast portion, its position is described by the kinematic equation:

$$H = h_1 + v_1 \tau_2 - \frac{1}{2} g \tau_2^2 \tag{2.11}$$

Note that the initial conditions, h_1 and v_1, come from the end of the powered lift-off. Substituting equations 2.7, 2.8, and 2.10 into equations 2.11 results in:

$$H = \frac{1}{2}(a_V - g)\tau_1^2 + \frac{(a_V - g)^2}{g}\tau_1^2 - \frac{1}{2}g[\frac{(a_V - g)}{g}\tau_1]^2 \tag{2.12}$$

which is an expression with τ_1 as the only unknown. Solving for τ_1 while grouping like terms yields the solution:

$$\tau_1 = t_{burn} = \sqrt{\frac{2gH}{a_V(a_V - g)}} \tag{2.13}$$

or the time the engines need to be on in order to coast to the desired height H. This means that the delta-V is given by:

$$dV = a_V t_{burn} \tag{2.14}$$

Thus, the delta-V cost in equation 2.14 is a function of the hover height and the takeoff vertical engine acceleration. Because the hover hop ascent is separate from its traverse, this script was run separately from that of the rest of the maneuver.

Powered Traverse

The powered traverse runs as long as the simulation time is less than t_{thrust}. It uses the two contributions to the engine acceleration. The first is due to the horizontal thrusters, and is defined as $a_H = (T_H/m)$. The second contribution comes from the vertical thrusters maintaining a hover by opposing the lunar gravitational field. In other words, $a_V = g_{lunar}$. These two accelerations are inserted in equation 2.5 to

generate the net engine acceleration vector necessary for state propagation.

Coast

The horizontal coast portion of the script runs until the vehicle's downrange position reaches d_{half} [8]. It is identical to the powered traverse except for the fact that the state is propagated with only $a_V = g_{lunar}$ as the engine acceleration. That is, during this phase the hopper is only thrusting against gravity as its momentum from the powered traverse carries it downrange.

Calculating final values

Recall that the two halves of a hover hop are assumed to be symmetric; the shape of the first half of the trajectory, as well as all of its performance data, should closely mirror that of the first [9]. Thus, to obtain overall performance metrics it is necessary to double the outputs. This is done in postprocessing.

2.2.4   Wrapper Script and Tradespace Generation

Each hop script also exists as a function, and these functions are utilized by the wrappers to run the simulations multiple times and create tradespaces. The ballistic hop function takes in T and t_{burn} as inputs, so the ballistic wrapper loops on these [10]. It takes in vectors of the two values and runs the simulation for each combination of elements. The outputs are matrices of the following:

- Delta-V (total and divided by components)

- Final mass

- Range

- Hop distance

---

[8]If the hopper passes d_{half}, the simulation stops and outputs an error message. This message contains the time at which it reached the halfway point.

[9]This is actually a conservative approximation since the vehicle mass will be lighter for the second half, so it will take less fuel to hover and descend.

[10]For the launch angle analysis in section 2.3.1.1, it also loops on launch angle.

38

- Landing velocity (horizontal and vertical components as well as the magnitude of their sum)

where matrix entry (a, b) corresponds to the a-th element of the T vector and the b-th element of the t_{burn} vector.

The hover wrappers work in a similar manner. The ascent version loops on vectors of T_V and H to output a matrix of delta-V, while its traverse counterpart loops on T_H and T_{thrust}. For the traverse, the output matrices are:

- First half Delta-V (for the powered traverse, the coast, and their sum)

- First half distance traveled (for the powered traverse, the coast, and their sum)

- Propellant mass consumed (during the powered traverse, the coast, and their sum)

- Velocity at the end of the powered traverse

Also, for ease of analysis, every thrust value was chosen such that it could be represented as an integer thrust-to-weight (T/W) ratio. This generalized the results as will be seen in section 2.3.

2.3 Results

2.3.1 Ballistic Hop

2.3.1.1 Launch angle analysis

If the ballistic hop was executed as an impulsive, instantaneous maneuver on a "flat" planet, the launch angle to achieve maximize range would be 45 degrees. However, this result might not be valid for the realistic situation where a non-impulsive maneuver is needed to execute the hop. To determine the optimal launch angle for the ballistic hop, trajectories were simulated while varying the launch angle and ascent thrust time. This process was carried out for various initial vehicle T/W to examine the effect of changes to the maximum engine thrust level. Figure 2-5 shows delta-V

costs versus launch angle, with contours representing a constant hop distance. The sequence of figures represent increasing engine T/W. The minimums on each curve reveal the most fuel-efficient launch angle. From the plots, it is seen that this optimal angle is in the range of 45 to 50 degrees.

From this analysis, it can be concluded that in order to maximize range for a given initial T/W, a launch angle of 45 degrees is approximately optimal for these non-impulsive hop trajectories. This 45 degree launch angle result will therefore be used for the rest of the ballistic hop study.

2.3.1.2 Delta-V analysis

With the optimal launch angle established, a more detailed look can be taken at the ballistic hop delta-V. Like the previous study, the ascent thrust time and initial T/W were varied parametrically to determine the hop range and delta-V cost.

Figure 2-6 is the most pertinent design plot. For a desired hop distance in meters, it shows the delta-V cost in m/s as a function of the initial T/W ratio. For a specific vehicle design, this information can be converted into propellant mass versus max engine thrust. Note that for short distances the cost is not very sensitive to thrust level. Thus, it can be concluded that smaller engines can be used for short-distance hops without incurring a significant fuel penalty. For longer hops, however, there is more of a fuel savings for using engines with a higher thrust capability.

Figure 2-7 looks at the data from a different perspective. This plot shows contours of constant hop distance as well, but this time they are plotted against takeoff thrust time and initial T/W. For a desired hop distance, the figure shows how long the engines need to thrust and the necessary thrust level. The vehicle can cover the same distance by either using a longer thrust time and a lower T/W, or by using a higher T/W but a shorter thrust time. The necessary range of thrust times increases for longer hops.

One final way of viewing the data is in Figure 2-8. This figure presents initial T/W curves plotted across hop distance in kilometers and delta-V values. As intuition would suggest, for a given delta-V budget, the vehicle can hop further with a larger
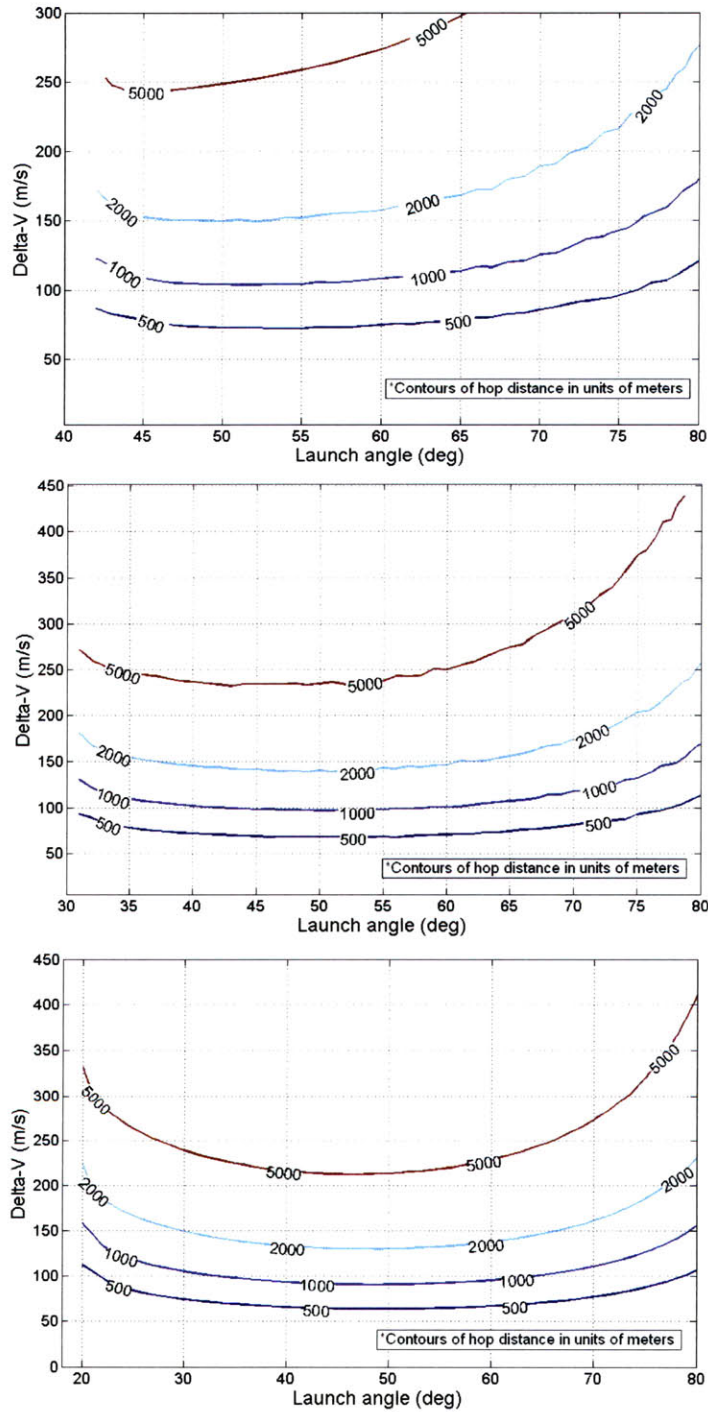
Figure 2-5: Hop distance as a function of launch angle and delta-V for T/W = 1.5 (top), 2.0 (middle), and 3.0 (bottom)
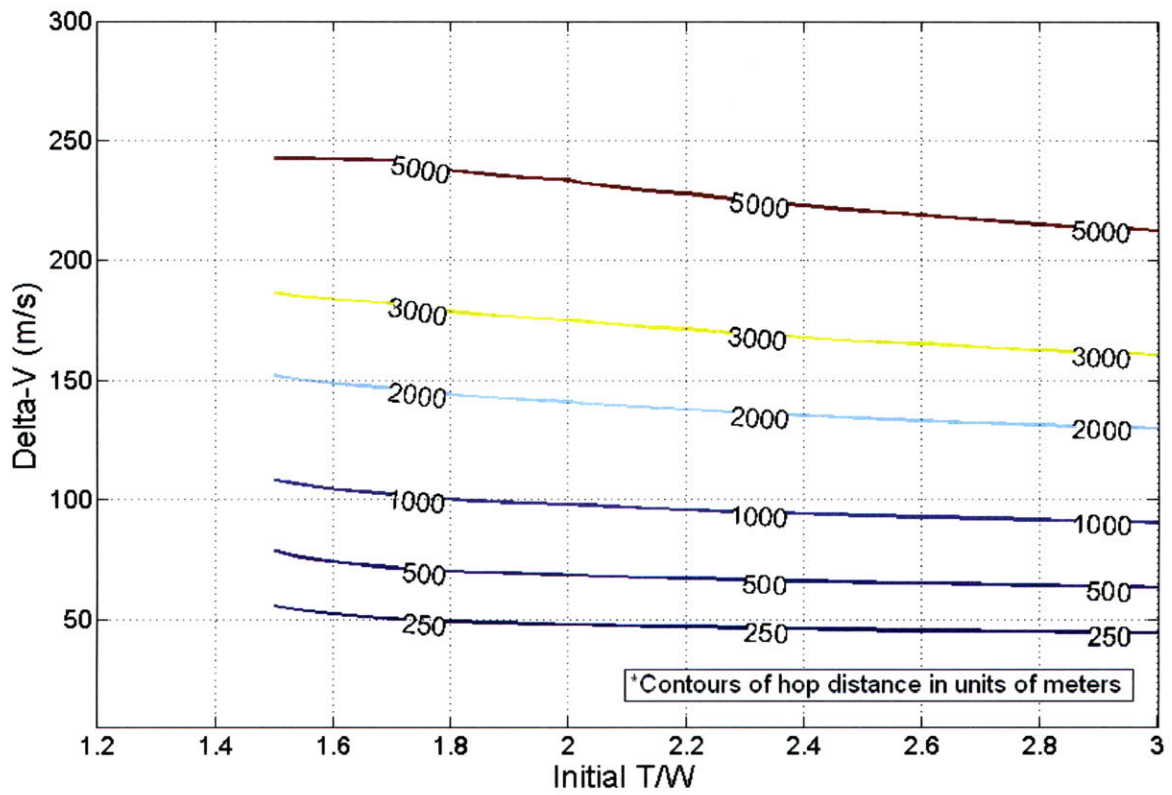
Figure 2-6: Hop distance as a function of initial T/W and delta-V
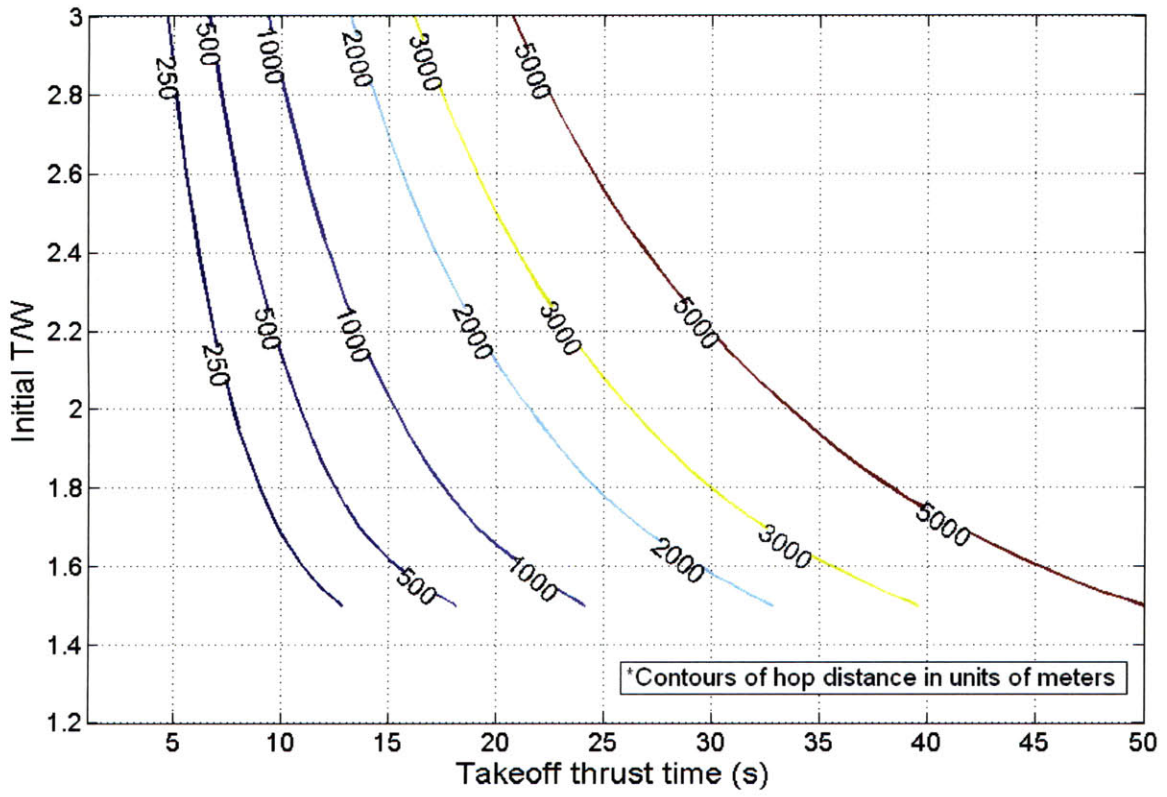
Figure 2-7: Hop distance as a function of takeoff thrust time and initial T/W
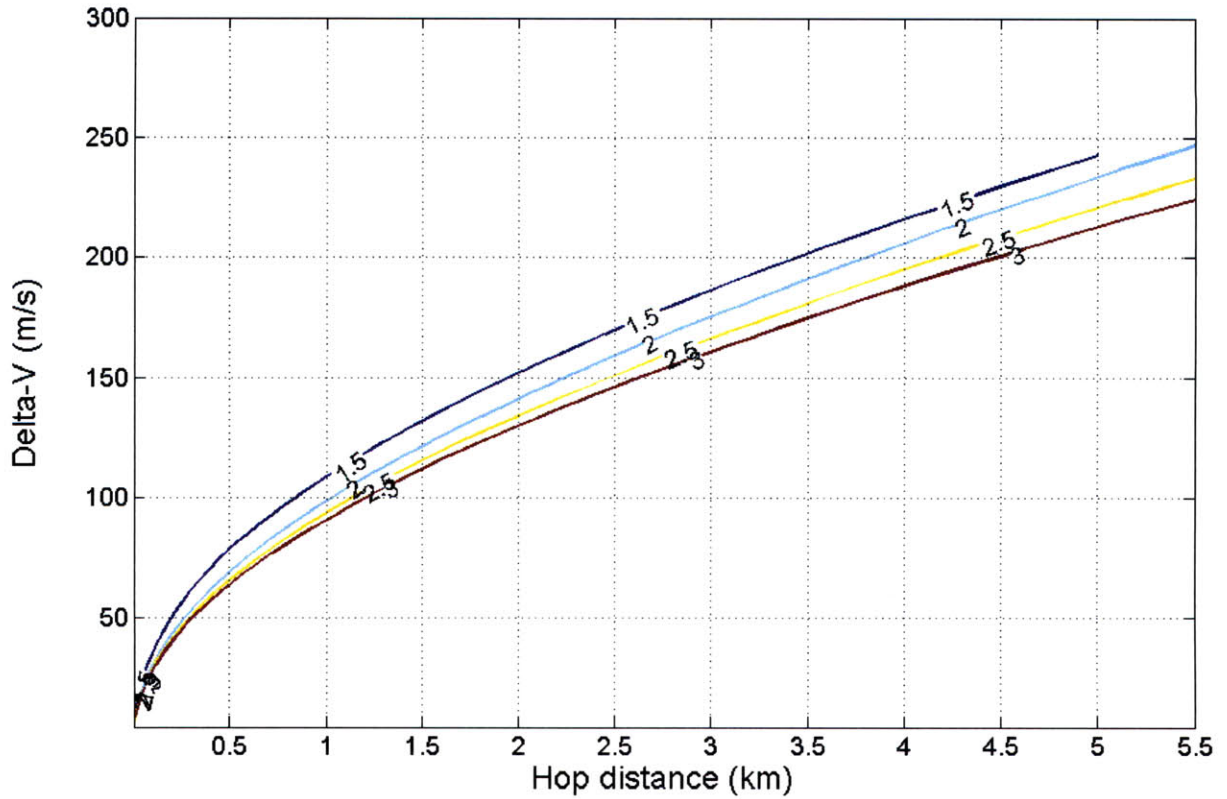
Figure 2-8: Initial T/W as a function of hop distance and delta-V

T/W ratio. Also, for a given distance, the delta-V cost decreases with increasing T/W.

2.3.2 Hover Hop

2.3.2.1 Ascent analysis

Figure 2-9 shows hover height contours plotted against T/W and the delta-V cost to reach that height. Recall that the ascent algorithm used here is fuel optimal. The figure shows that for a larger initial T/W, the cost to reach a given height decreases, i.e. with a small takeoff thrust the engines must say on longer. More fuel is expended in order to reach larger hover heights.
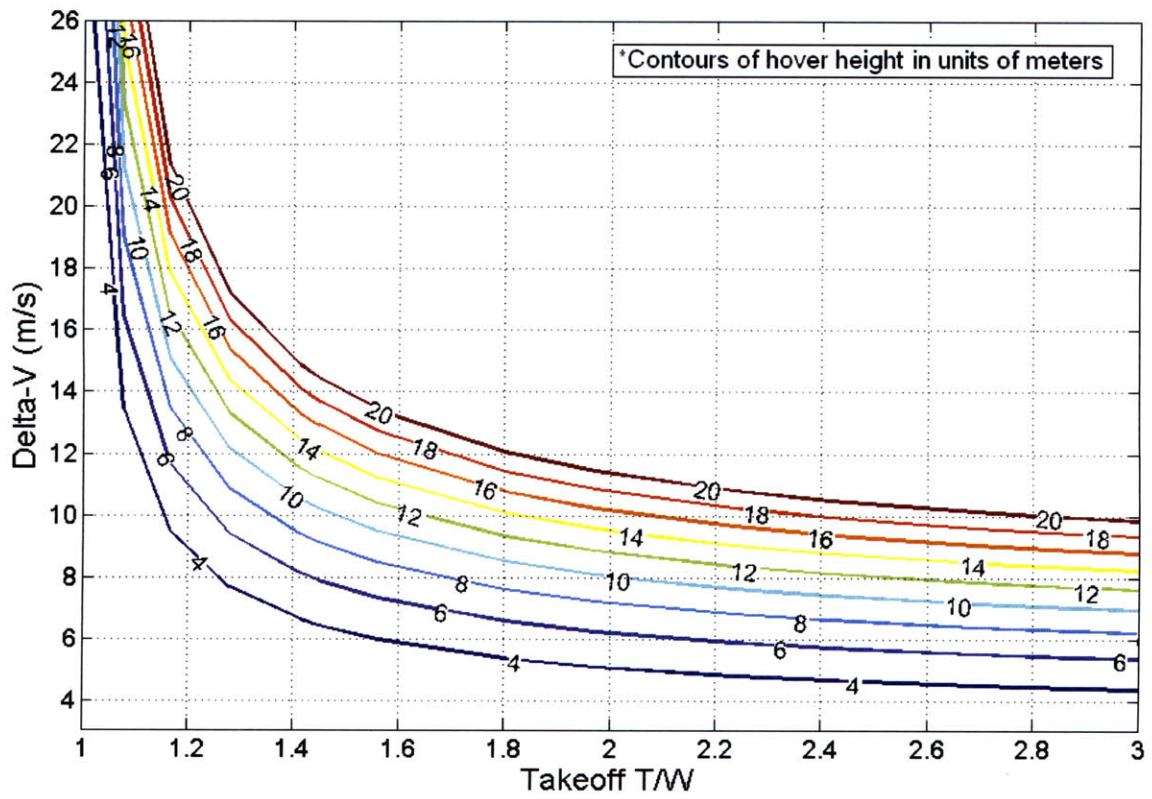
Figure 2-9: Hover height as a function of initial T/W and delta-V

2.3.2.2 Delta-V analysis

Once the vehicle has reached the desired height, the horizontal traverse phase begins. While providing vertical engine thrust to counter gravity and maintain altitude, the vehicle accelerates horizontally toward the target, coasts, and then decelerates to a stop above the target. The two traverse distances examined, 500 meters and 5000 meters, were chosen since they are the bounds on the X-PRIZE hop. Figure 2-10 shows the delta-V cost for the full traverse plotted against the thrust time to start the horizontal traverse for various horizontal engine thrust levels. These thrust levels were chosen such that they corresponded to initial T/W values of the vehicle. Note that thrusting against gravity is also included in these costs [11].

For low horizontal thrust levels, the delta-V cost of the mission increases dramatically as thrust time decreases. This is intuitive—the vehicle is spending more time both moving downrange and opposing gravity. Notice that the curves have minimums [12]; these represent the optimal delta-V balance between thrusting horizontally and thrusting against gravity, implying that keeping the horizontal engines on for the entire traverse is not fuel-optimal.

Figure 2-11 presents just these minimum delta-V points for the 500m and 5000m cases. The minimum delta-V remains fairly constant for T/W values greater than 0.5, which implies that horizontal engines that produce T/W above 0.5 do not provide any fuel savings. Very small engines, in contrast, will be very costly in terms of delta-V.

2.3.2.3 Mission time analysis

One could imagine a scenario in which delta-V and fuel are not the dominant constraints in a mission. Perhaps a situation could arise in which the goal is to minimize the time of the hover hop. Figure 2-12 plots full traverse mission times against first-half thrust times for various T/W ratios for the horizontal engines.

The curves here look similar to the delta-V plots presented earlier. The main

---

[11] Also, note that the maximum thrust time for each curve occurs at the midpoint of the particular traverse. This end-point case is a scenario where the horizontal engines accelerate the vehicle continuously to the halfway point and then decelerate the vehicle for the second half.

[12] Not all pictured on the 5000m plot, but it follows the same form as its 500m counterpart.
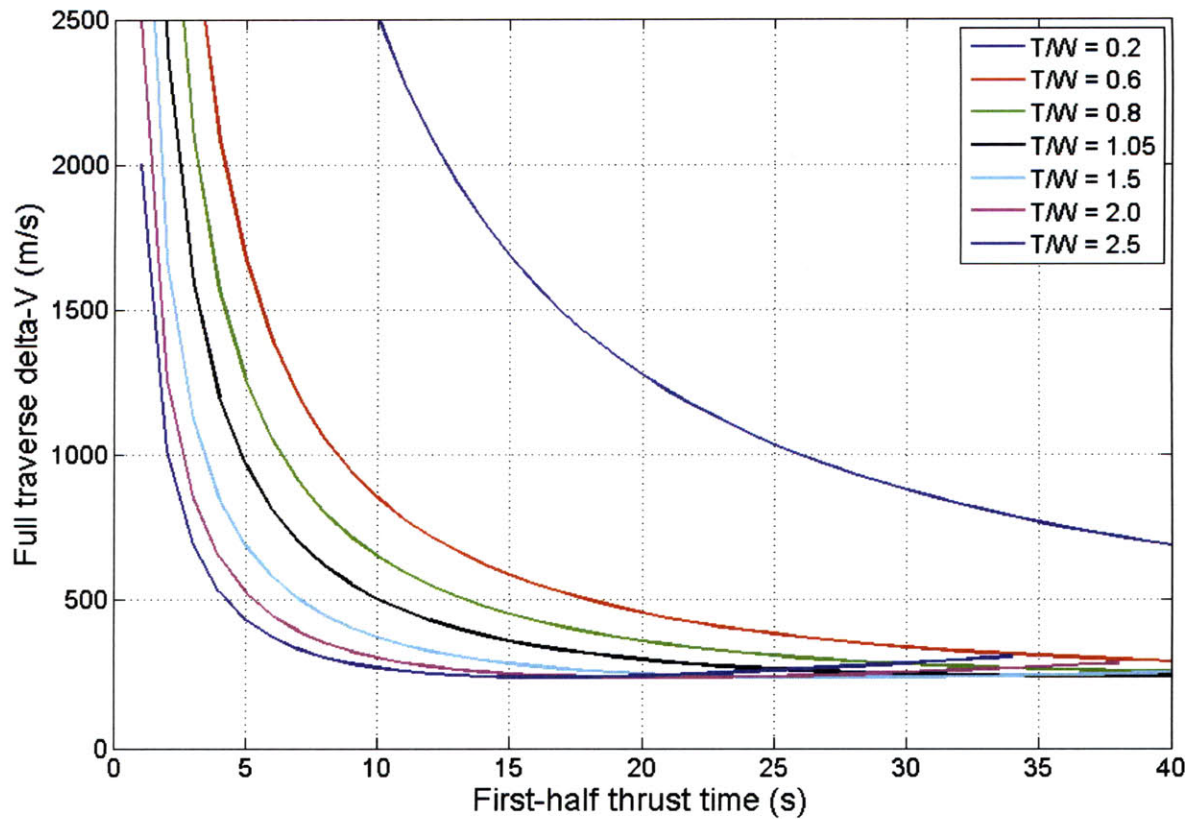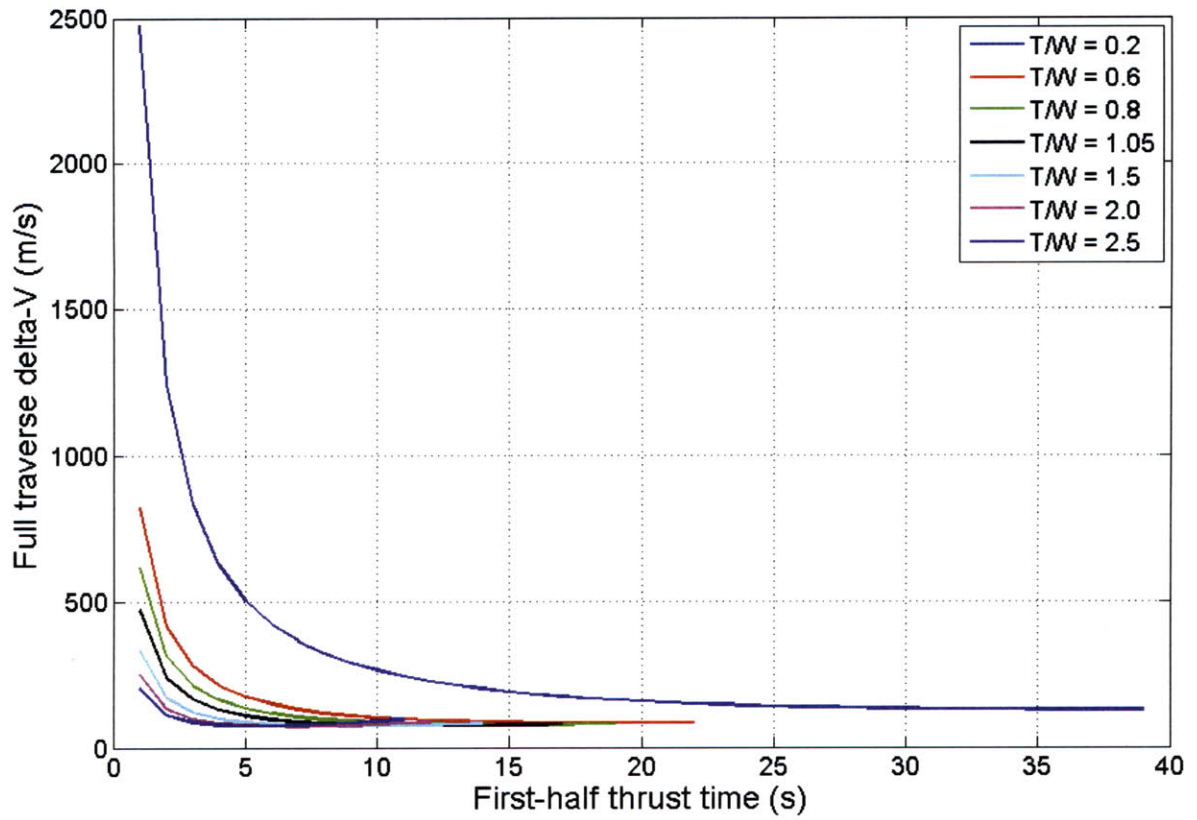
Figure 2-10: Full traverse delta-V as a function of first half thrust time for 500m (top) and 5000m (bottom)
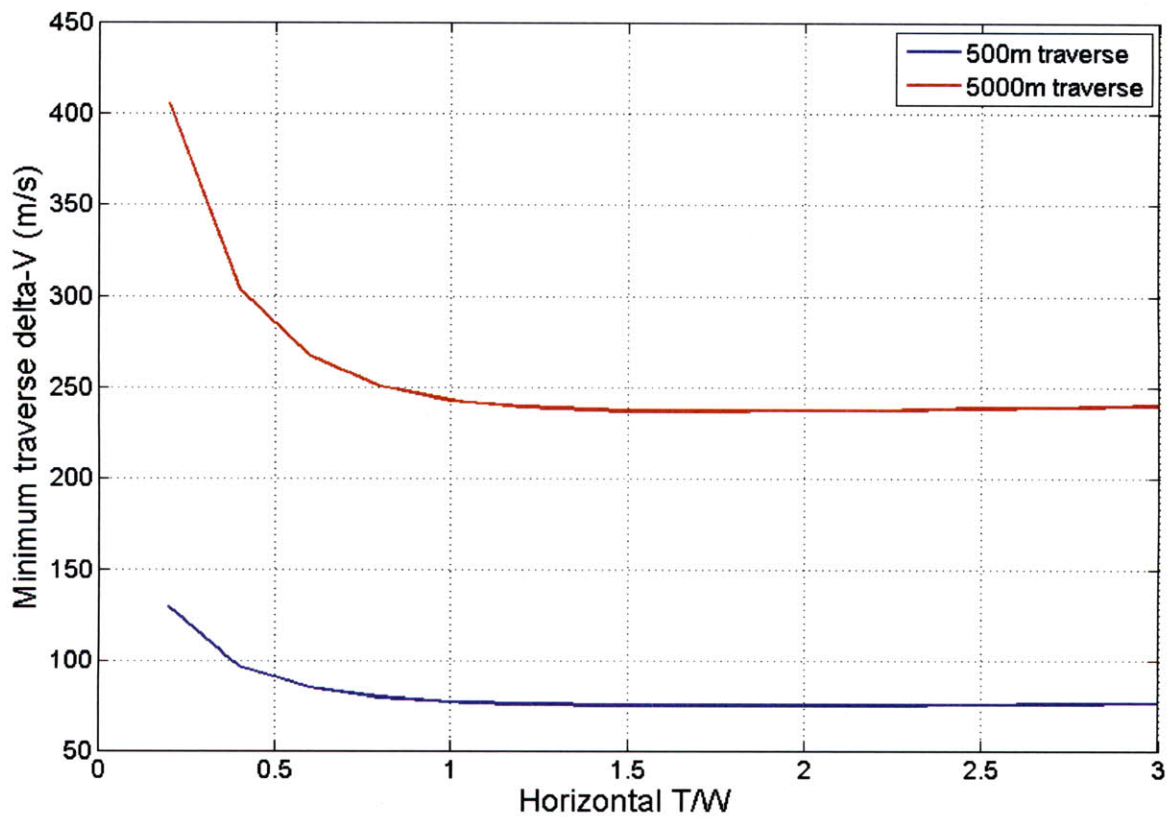
Figure 2-11: Minimum traverse delta-V for varying T/W ratios
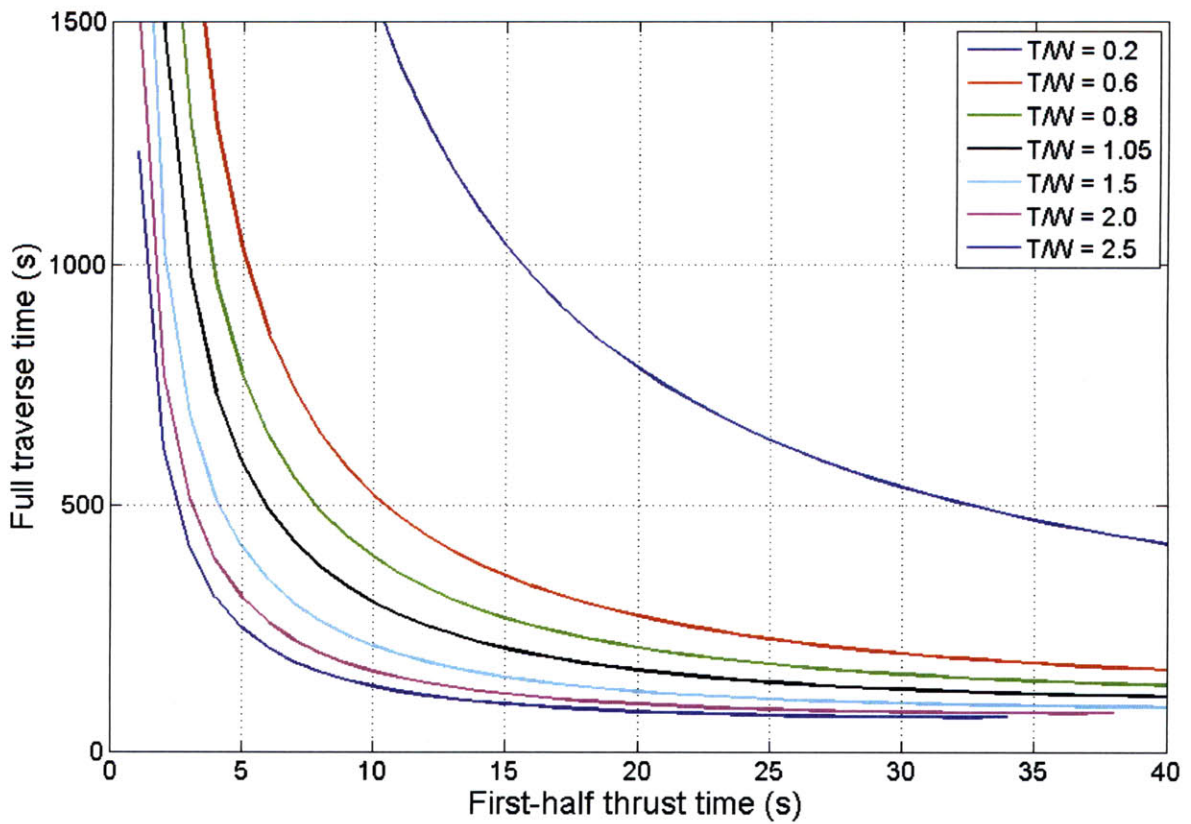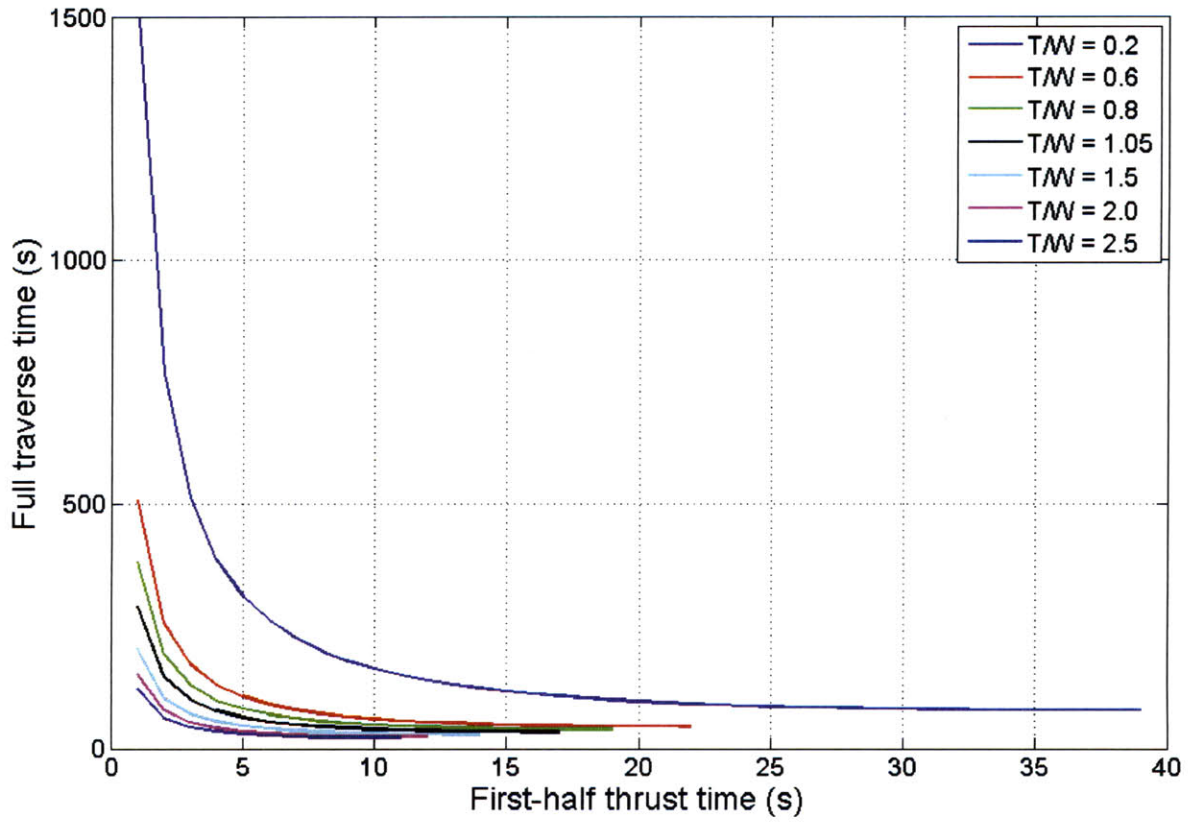
Figure 2-12: Full traverse time as a function of first half thrust time for 500m (top) and 5000m (bottom)

49
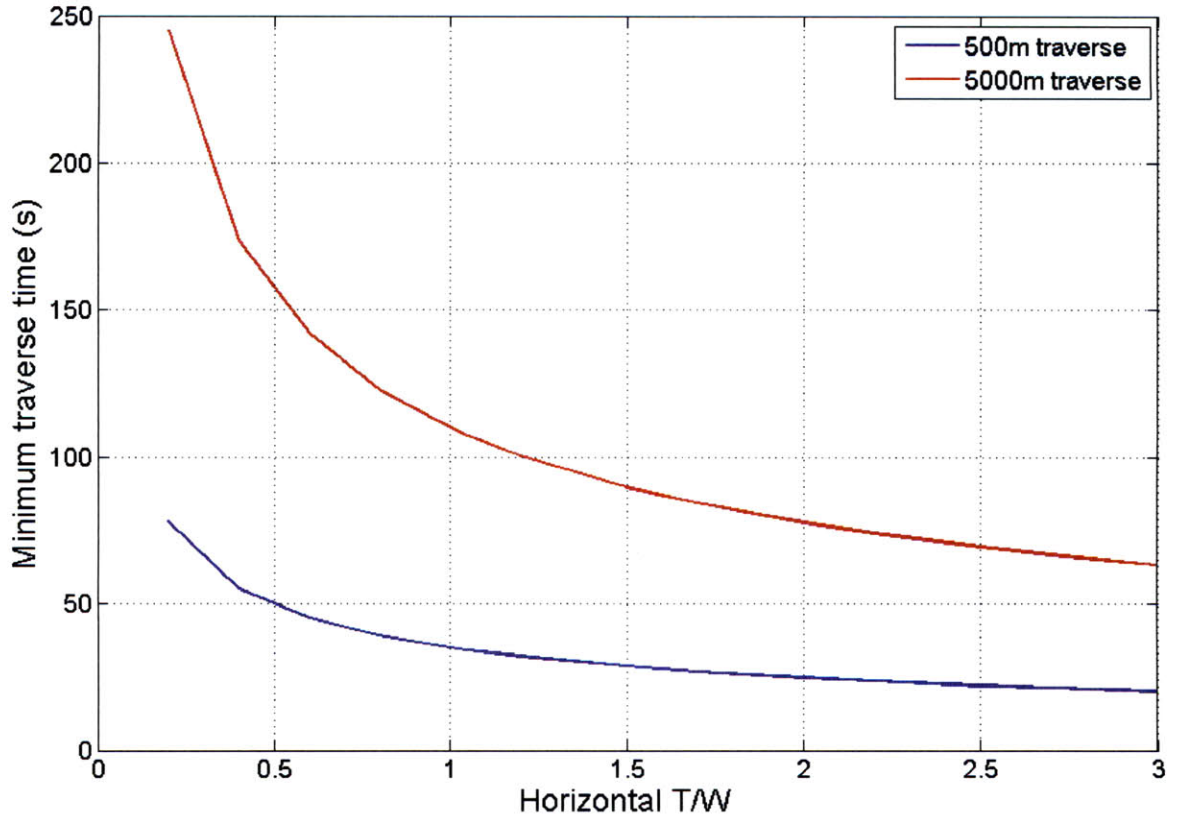
Figure 2-13: Minimum traverse time for varying T/W ratios

difference is that, unlike with delta-V cost, the curves monotonically decrease. In other words, to minimize traverse time the vehicle should accelerate continuously for the entire first-half and decelerate continuously for the entire second-half of the traverse. Figure 2-13 shows these minimums explicitly. As expected, the minimum traverse time decreases as the thrust increases.

It is interesting to note that the minimizing traverse delta-V does not minimize traverse time, and vice versa. Figure 2-14(top) shows the full traverse time corresponding to using the minimum delta-V values, while figure 2-14(bottom) is a plot of the delta-V required for the minimum time traverse.

It is evident that these curves are not the same as those in figures 2-13 and 2-11 mentioned earlier. Since there is a tradeoff between minimizing traverse delta-V (fuel) and traverse time, a weighted optimization would be needed if both were deemed critical mission parameters.
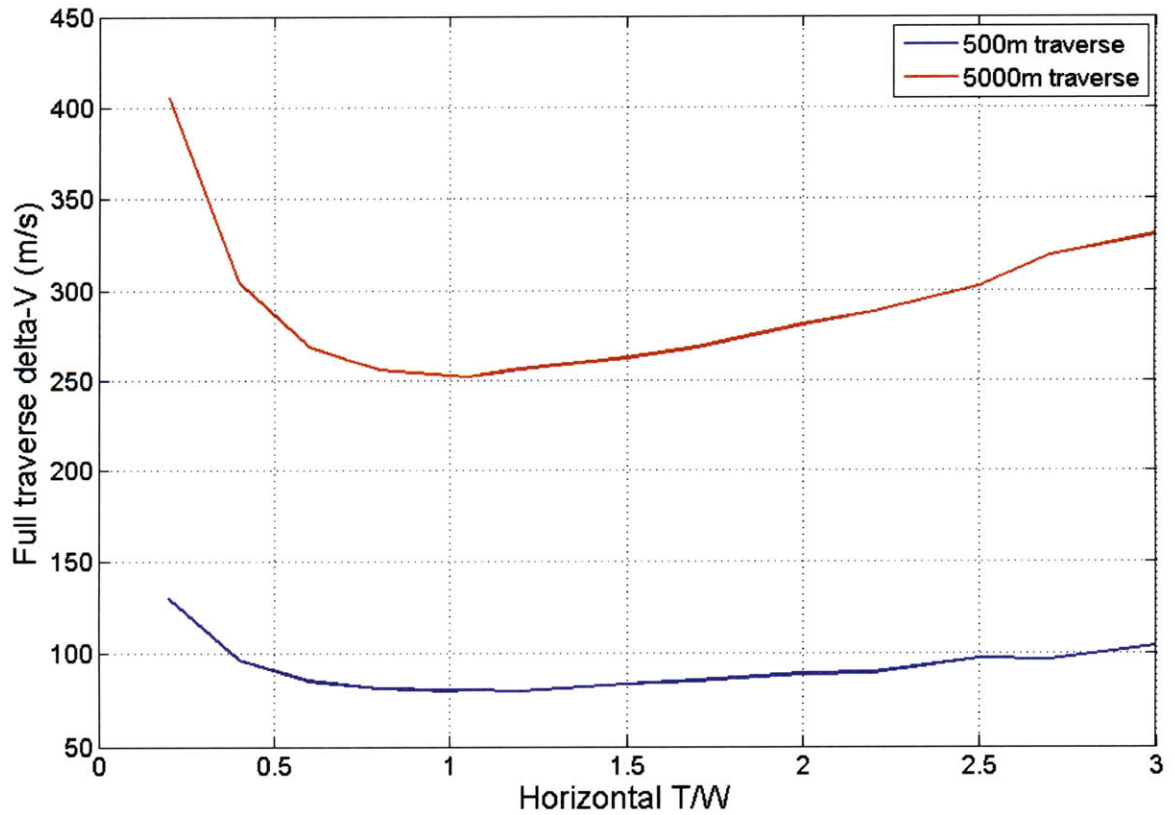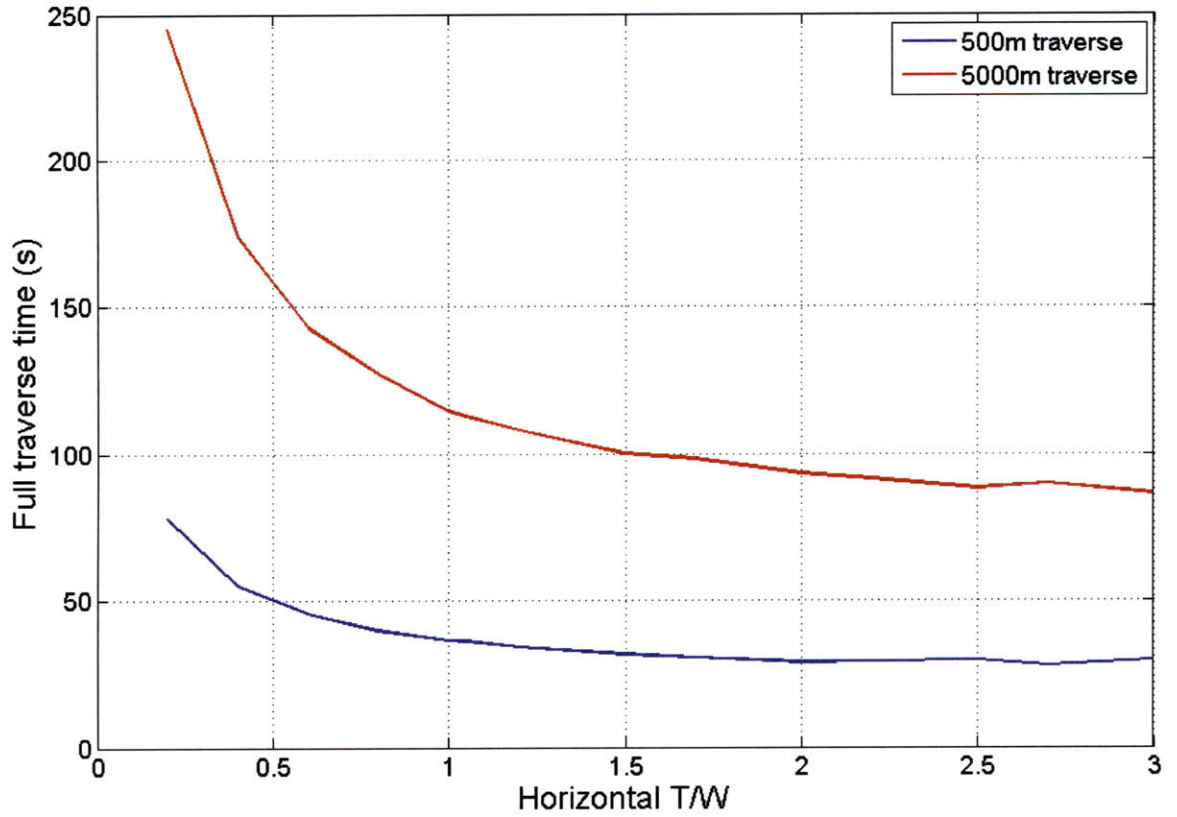
Figure 2-14: Full traverse time required for minimum delta-V traverse (top) and delta-V required for minimum time traverse (bottom) for various T/W ratios

51

2.3.3 Ballistic and Hover Comparison

With the hop methods analyzed, it is now appropriate to compare the two with respect to their delta-V costs. Figure 2-15 looks at the optimal delta-V costs of the 500m and 5000m hop distances for both the ballistic and hover hops [13].

The total delta-V cost for a hover hop is a function of not only the traverse, but also the height of the hover and the thrust capability of the ascent and descent engines. This is illustrated by the multiple curves for each hop distance in figure 2-15(bottom). The theoretical "no hover" case, which is only a traverse, has a comparable fuel cost to that of its ballistic counterpart. However, the ascent and descent ultimately add to this cost. The dotted curves show trends: hop cost increases with hover height, but if height is held constant then less delta-V is required for higher takeoff T/W values. This fact will make the hover maneuver the more fuel expensive of the two trajectories.

Thus, the data shows that the ballistic hop maneuver is more delta-V efficient than its hover counterpart. Nevertheless, this does not give immediate grounds to conclude that the ballistic hop will always be the better option. It is necessary to relax the initial assumptions in section 2.1.3 and consider a number of operational issues surrounding each hop.

A true ballistic hop is an idealization. In reality, a vehicle will have to lift off the ground before it enters into the ballistic trajectory. In the case where it only has downward pointing main engines for delta-V execution, it not only will have to perform this lift off but it will also have to reorient the thrust vector appropriately to create lateral motion. Aside from costing extra fuel, it also adds complexity to the maneuver. The vehicle would then need to use its reaction control jets to change its attitude during the ascent and during the decent maneuver such that it lands with the proper orientation.

The hover hop as analyzed is also somewhat of an ideal case. If the vehicle design provides both horizontal and vertical engines of sufficient thrust capability, this hop

---

[13]For Figure 2-15(bottom), "Initial T/W" is with respect to the horizontal engines only, but remember that the delta-V cost includes the 1 T/W thrusting of the vertical engines.
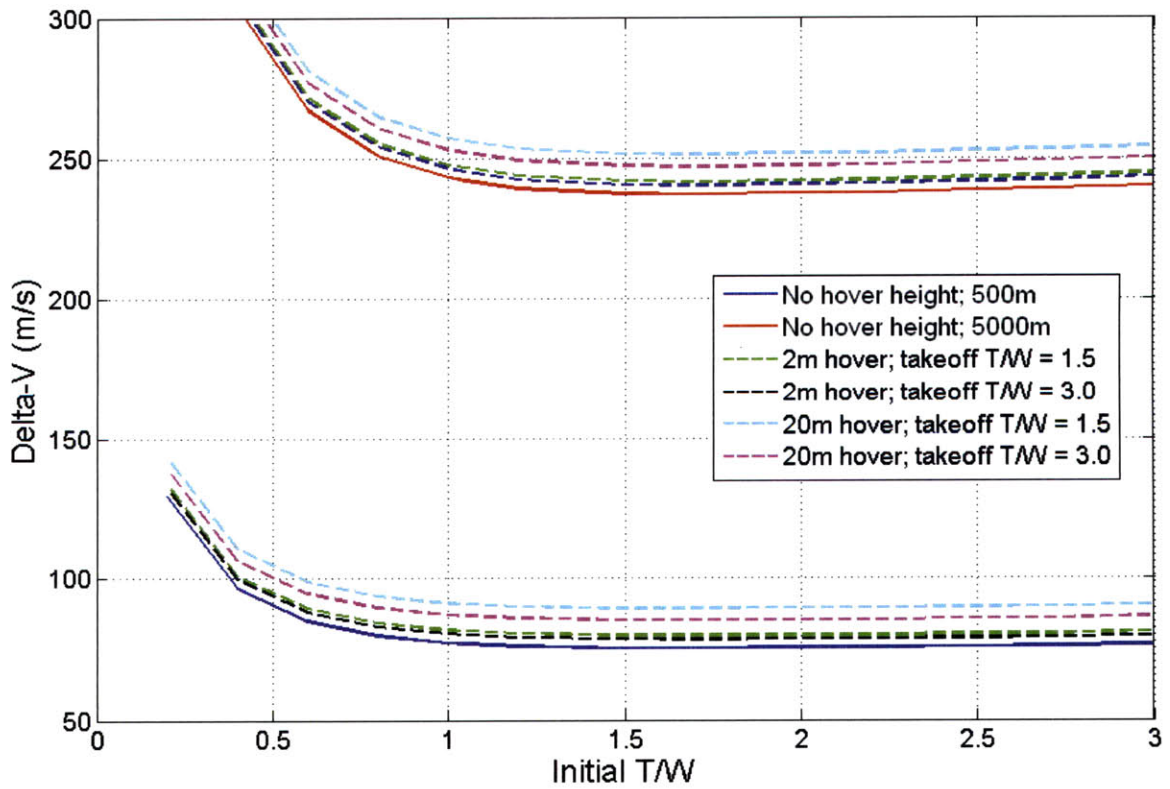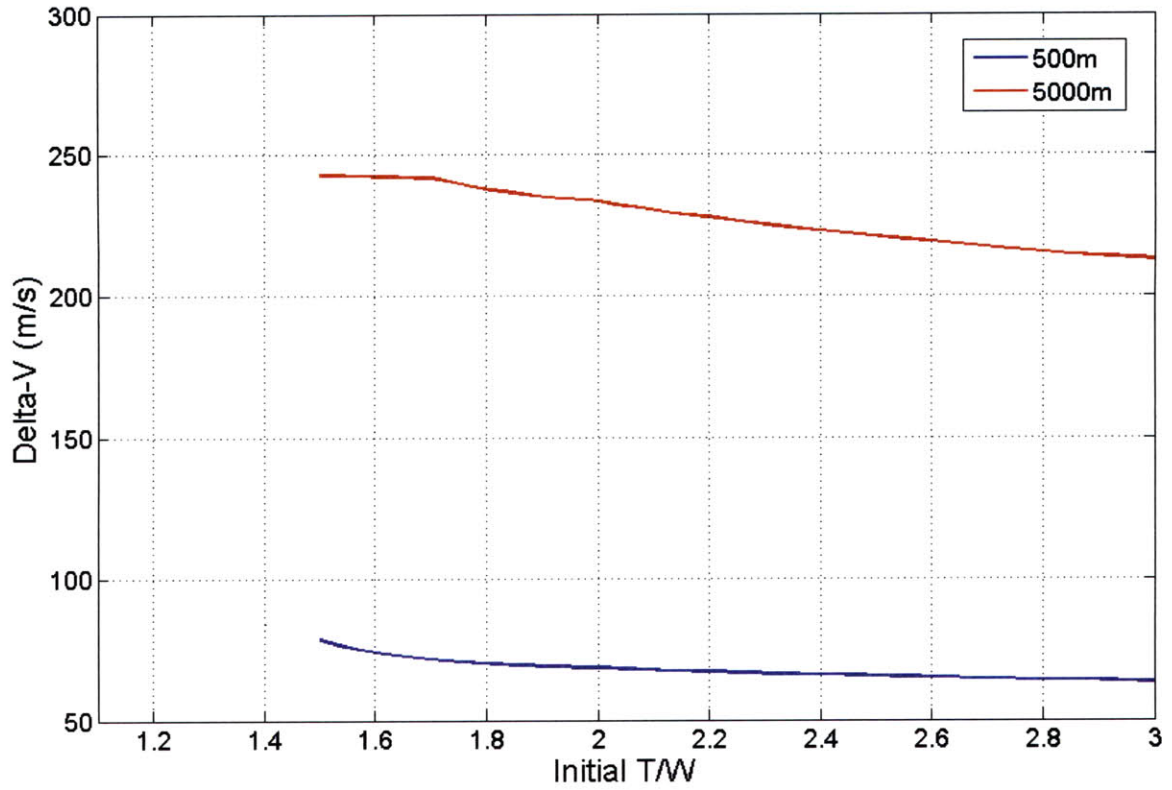
Figure 2-15: Ballistic (top) and hover hop (bottom) delta-V cost comparison for 500 and 5000m hop distances

can be executed as a fixed-attitude maneuver. However, if the vehicle is designed with only downward pointing main engines for delta-V execution, the vehicle will have to rotate as it goes from the ascent to traverse phases in order to create lateral motion. The same will be necessary to transfer between the traverse and the descent.

There are also guidance and navigation factors. For a ballistic hop, precise attitude control and delta-V execution is critical since the maneuvers are relatively brief compared to the entire hop duration. In contrast, since the engines are on for the entire duration of a hover traverse, the vehicle will have significant time to correct small dispersions that occur along the trajectory. The hover hop also allows for the use of lower thrust engines than is feasible for the ballistic hop [14].

Tradeoffs still exist if fixed attitude maneuvers are possible. For example, communication systems or sensors collecting surface data might require a fixed attitude, and/or a fixed altitude to operate. For the hover hop, the engines are always on, which may create vibrations that disrupt or degrade communication or surface data collection activities. The ballistic hop has an advantage here: the trajectory could be designed such that it performs all attitude maneuvers near the beginning and end of the flight, leaving a powerless coast phase free of vibrations. Also, due to the high altitudes obtainable with this hop, any imagery hardware will be free from the potential ground effects caused by a low altitude hover hop.

Nevertheless, for TALARIS and NGL, one of the major design drivers is ease of testing. The precision necessary to perform a ballistic hop increases the probability of catastrophic failure: if the hopper is unable to orient itself properly for a landing, it will crash. From a testing standpoint this means resources must be allocated to purchase new parts and rebuild the hopper. This is not possible with the limited budget of the TALARIS project. As such, the hover hop offers significant advantages: it can be run with a fixed attitude and with degrees-of-freedom constrained. This reduces the chance of a failure seriously damaging the vehicle.

---

[14]Closer to $T/W = 1$.

2.4 Hop Analysis Conclusion and Takeaways

The Hop Tradespace Tool was designed to investigate the performances of the two fundamental hop types: the ballistic and hover. At the end of this first-order analysis it was determined that from a fuel standpoint, the ballistic hop is the most efficient. However, other factors must be taken into account such as guidance and navigation difficulties, operations, and most importantly for the TALARIS project, ease of testing. It was for this reason that the hover fuel penalty was accepted and the hover hop was deemed to be the best option for the current project. The next chapter will use a modification of the HTT to investigate the specific performance of a TALARIS hover hop.

THIS PAGE INTENTIONALLY LEFT BLANK

Chapter 3

Preliminary TALARIS Mission Analysis

Building off of Chapter 2, this chapter uses the tool developed and specifically applies it to the TALARIS vehicle.

3.1   Review of TALARIS Mission

As mentioned in Chapter 1, TALARIS is being constructed at MIT as a 1-g testbed for lunar hopper software. When completed it will be presented in demonstration to the project's various stakeholders. This raises questions on what exactly needs to be shown. That is, how long does the demo need to run to prove to the stakeholders that the vehicle works? This problem can be reworded from a more technical standpoint. Specifically, what are the bounds on vehicle performance and will this be enough to prove that TALARIS is functional?

A baseline hop has been proposed to answer these questions. It consists of a 30 meter traverse with a net 70 N of thrust from any pair of horizontal thrusters, and these thrusters fire for an initial two seconds to start the vehicle moving downrange. No hover height is specified. It is necessary to evaluate this baseline with respect to its feasi bility and suggest possible alternatives if needed.

Analyzing trajectories and looking for bounds on performance requires running

various simulations of a hop while changing parameters. Conveniently, the HTT was designed for such a task. Thus the solution to the above questions is to utilize this tool to create a TALARIS mission tradespace.

3.2 TALARIS Mission Tradespace Tool

The TALARIS mission tradespace study utilizes the HTT and as such delivers first-order results with the assumptions listed in Chapter 2.1.3. Recall that unlike the generic lunar hopper, TALARIS operates on Earth and uses the EDF system to simulate lunar gravity. As such, the HTT's hover tool had to undergo a number of modifications in order to perform this analysis.

3.2.1 Initialization Modifications

The following parameters were modified or added to the initialization section of the hover tool:

- Propellant mass, $m_{prop} = 4.7$ kg; the projected mass of the vehicle's fuel (nitrogen).

- Dry mass, $m_{dry} = 45.0$ kg; the projected mass of the vehicle's structure.

- TALARIS frontal area, $A_{TAL} = 0.312$ m^2; the approximate frontal area of the first TALARIS structure.

- TALARIS overhead area, $A_{TOP} = 0.403$ m^2; the approximate area of the top of the first TALARIS structure.

- Rectangular coefficient of drag, $C_d = 1.05$; used to approximate the C_d for TALARIS.

- Specific impulse, Isp = 46.28 seconds; the initial Isp for the CGS thrusters.

- Max CGS ascent thrust, $T_{CGS_{asc}} = 200$ N; Maximum net thrust from vertical CGS thrusters.

- CGS hover (vertical) thrust, $T_{CGS_V} = (\frac{1}{6} \cdot m \cdot g_{earth})$ N; Nominal thrust required for the CGS to keep the vehicle hovering.

- Required EDF thrust, $T_{EDF} = (\frac{5}{6} \cdot m \cdot g_{earth})$ N; the thrust required from the EDFs to simulate a lunar environment.

The following are the user-defined inputs:

- Max CGS traverse (horizontal) thrust, T_{CGS_H}(N)

- Initial horizontal thruster burn time, t_{burn}, (s)

- Half of the traverse distance, d_{half} (m)

- Hover height, H_{hover}(m)

Since the TALARIS flight will take place on Earth, the modified HTT also includes different environmental parameters in order to model aerodynamic forces:

- Earth $\mu = 398.6 \times 10^{12}\ m^2/s^3$

- Radius of Earth, $R = 6371.0 \times 10^3$ m

- Earth g = 9.81 m/s^2

- Density of air, $\rho = 1.20$ kg/m^3

3.2.2   General Equations

The equations used in the TALARIS version of the HTT are, in general, the same as those used in Chapter 2. The first modification is present in the equation of motion. It is now written as:

$$\ddot{\mathbf{r}} = \vec{\mathbf{a}}_{grav} + \vec{\mathbf{a}}_{eng} + \vec{\mathbf{a}}_{drag} \tag{3.1}$$

where $\vec{\mathbf{a}}_{eng}$ can be broken down into:

59

$$\vec{a}_{eng} = (\vec{a}_{EDF} + \vec{a}_{CGS_V} + \vec{a}_{CGS_H}) \tag{3.2}$$

The engine acceleration component is now explicitly broken into three parts. The first, $\vec{a}_{EDF}$, is due to the EDFs creating the simulated lunar gravity field. It is always defined as:

$$\vec{a}_{EDF} = (5/6)g_{earth}\hat{\mathbf{U}}\mathbf{P} \tag{3.3}$$

or $5/6$ of the Earth's gravitational acceleration. The next two engine accelerations, $\vec{a}_{CGS_V}$ and $\vec{a}_{CGS_H}$, are the contributions from the vertical and horizonal cold gas thrusters. Due to the assumption that the vehicle says in one plane of motion, they can be rewritten as follows:

$$\vec{a}_{CGS_V} = a_V\hat{\mathbf{U}}\mathbf{P} \tag{3.4}$$

$$\vec{a}_{CGS_H} = a_H\hat{\mathbf{D}}\mathbf{R} \tag{3.5}$$

The final acceleration was not present in the lunar simulation and comes from drag. It is calculated from:

$$\vec{a}_{drag} = -\frac{F_{drag}}{m}\frac{\vec{\mathbf{v}}}{|\vec{\mathbf{v}}|} \tag{3.6}$$

where m is the current mass, $\vec{\mathbf{v}}$ is the velocity vector relative to the atmosphere, and F_{drag} is the force of drag. The drag force is calculated via:

$$F_{drag} = \frac{1}{2}\rho(\vec{\mathbf{v}} \cdot \vec{\mathbf{v}})C_dA \tag{3.7}$$

and uses the constants from section 3.2.1. The value of the area A depends on the direction of motion.

Lastly, the mass rate equation is now written as:

a_V [m/s^2]	$T_{CGS_{asc}}/m$
a_H [m/s^2]	0
A[m^2]	A_{TOP}

Table 3.1: Hover hop ascent values

$$\dot{m} = \frac{-(T_{CGS_H} + T_{CGS_V})}{Isp \cdot g_{earth}} \qquad (3.8)$$

The distinction between the CGS and EDF thrusts must be made due to the fact that the fans are air breathing and do not consume fuel.

3.2.3 Simulation Modifications

Ascent

TALARIS will not be using the idealized ascent discussed in Chapter 2. Although its specific method has yet to be finalized, this analysis will assume that a closed-loop PID controller will be utilized to get the hopper to its target height. Before the ascent begins, the EDFs will already be ramped up to the proper revolutions per minute (RPMs) which generate thrust equal to 5/6 of the vehicle's weight. The vertical CGS thrusters will then turn on feeling a lunar environment, and using feedback and the PID controller, will ascend to the specified height.

The ascent phase of the script runs until the vehicle settles at its target height, where "settling" is defined as the altitude stabilizing within 0.01m of that target. It begins by calculating the current T_{EDF} since it is a function of total vehicle mass. $T_{CGS_{asc}}$ is initialized to zero. The net engine thrust is therefore $T_{asc} = T_{CGS_{asc}} + T_{EDF}$. Equations 3.4, 3.5, and 3.7 are then completed with the values listed in table 3.1. This results in the acceleration necessary to propagate the state. Feedback from the controller is used to increment $T_{CGS_{asc}}$ appropriately at each timestep. The mass is updated using equation 3.8 with T_{CGS_H} set equal to zero.

	Powered Traverse	Coast	Brake
a_V [m/s^2]	T_{CGS_V}/m	T_{CGS_V}/m	T_{CGS_V}/m
a_H [m/s^2]	T_{CGS_H}/m	0	$-(T_{CGS_H}/m)$
End condition	t_{burn} is reached	Part 1: d_{half} is reached Part 2: Part 1 distance traversed	Horizontal velocity = 0

Table 3.2: Accelerations and end conditions for hover hop phases

Powered Traverse, Coast, and Powered Brake

The remainder of the hop phases can be described by their engine accelerations. Table 3.2 lists these values. The current tool uses a constant T_{CGS_H} whereas T_{CGS_V} is updated at each timestep. The simulation inserts the accelerations into equation 3.1 to propagate the state at each phase. Note that the area used for the drag equation is A_{TAL}.

Descent

As was the case with the lunar analysis in Chapter 2, it is assumed that the descent will be similar in profile to the ascent. As such it is not a part of the simulation and is factored in during postprocessing.

3.3   Results

Recall that the baseline hover hop contains a 30 meter traverse, 70 N of horizontal thrust, and a two-second powered thrust time to begin the traverse. The results of the baseline traverse are:

- Peak velocity: 2.83 m/s

- Traverse time: 12.80 seconds

- Fuel consumed: 2.80 kg

- Distance actually traveled: 29.40 meters [1]

---

[1] Due to the setup of the simulation, drag prevents the vehicle from reaching the desired traverse
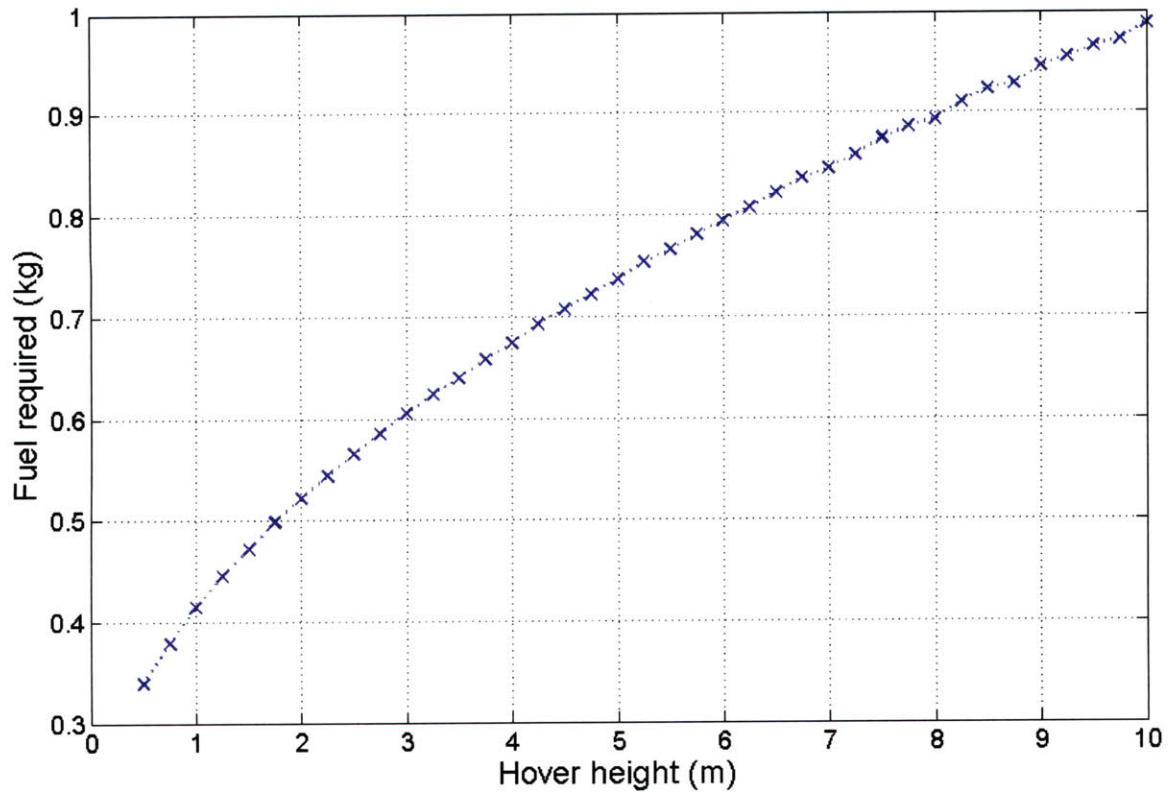
Figure 3-1: Fuel consumed during the ascent for various hover heights. The blue dotted line represents trends.

The question is if a traverse with these characteristics could be part of a complete TALARIS hop. The primary constraint is the fuel required. The 2.80 kg of propellant used by the baseline traverse is indeed within the alotted 4.7 kg available, but in reality, the amount of *useable* fuel is only about 3.64 kg [2]. To create a buffer to allow for uncertainty, this is reduced by 10% resulting in only 3.28 kg available. The traverse fuel cost is still within this budget. However, a complete hop contains an ascent and descent as well. Thus the baseline traverse leaves about 0.48 kg of fuel for the other two hop phases.

Figure 3-1 shows if 0.48 kg is enough to complete an ascent and landing. The figure depicts the fuel necessary to settle at a given height using the PID controller

distance. In practice, a guidance algorithm would most likely control the thrusters in order to compensate for this effect.

[2] This is due to the physics of the cold gas propulsion system.

63

Traverse distance (m)	Traverse fuel (kg)	Max ascent and descent fuel (kg)	Max hover height (m)
30	2.80	0.48	< 0.50
25	2.50	0.78	0.75
20	2.20	1.08	2.00
15	1.90	1.38	4.00
10	1.60	1.68	6.75

Table 3.3: Traverse distances and maximum hover heights

[3]. If the conservative assumption is made that the ascent and descent are symmetric, only about 0.24 kg of fuel can be used for the ascent. This corresponds to a maximum allowable hover height of under 0.5 meter. This is not reasonable; it leaves no room to try other heights, and it almost certainly will subject the hopper to ground effect. Thus, the baseline hop must be redesigned.

Table 3.3 shows various traverse distances with their corresponding fuel and maximum hover height. Intuitively, the 10 meter traverse distance has the most fuel available for an ascent and descent and thus can fly higher off the ground. However, TALARIS will not be hovering this high during its initial demos, and as such allocating fuel for a approximately 7-meter hover would not be an efficient use of mass. A more realistic hover height is 2-meters; not only is this reachable on the original 2.5 meter tall TALARIS test stand, but this is the height that is assumed to be free of ground effects while minimizing the damage should the vehicle lose power and fall. A 20-meter traverse is the maximum possible for this height, but it does not leave any room for error. This leaves the 15-meter traverse as the most appropriate of these choices. Therefore the new baseline is now:

- Hover height: 2.0 meters

- Traverse distance: 15.0 meters

- 70N traverse thrust with initial 2-second thrust time

The results from this new traverse are:

---

[3]For each height, the gains are tuned as to only have 0.01 meter maximum overshoot.

- Peak velocity: 2.81 m/s

- Traverse time: 7.26 seconds

- Fuel consumed: 1.90 kg

- Distance actually traveled: 14.70 meters [4]

And for the entire hop:

- Fuel consumed: 2.94 kg

- Useable fuel remaining: 0.70 kg

- Hop time: 13.08 seconds

This trajectory will show that TALARIS can perform a hover hop while staying within the bounds of its capabilities.

Tradespace Study: Constant Traverse Distance

As with the general case in Chapter 2, it is useful to run the traverse simulation across a number of parameters to discover trends. Keeping the desired traverse distance constant at 15 meters, the net horizontal thrust was chosen to be 50 N, 70 N, and 100 N as the burn time was varied between one second and the maximum burn time for that thrust level [5]. A MATLAB wrapper was configured to run these cases with the simulation. Figure 3-2 plots initial burn time across fuel consumed for the three different thrust levels.

The trends are similar to that which were seen in Chapter 2. Each thrust curve has a minimum, representing the optimal balance between using fuel to thrust against gravity and having to slow the vehicle's initial momentum. Two features stand out. First, none of these thrust levels violate the fuel constraint with any burn time; they all have a fuel cost of less than 3.0 kg [6]. And secondly, the baseline burn time of two

---

[4]See footnote 1.

[5]The maximum burn time is that which brings the vehicle to the traverse midpoint, which is 7.5 meters in this instance.

[6]Of course, this does not mean they are all capable of reaching the same hover heights.

Figure 3-2: Traverse fuel used as a function of initial horizontal burn time for various thrust levels. The green dot represents the baseline case.

Figure 3-3: Total traverse time as a function of initial horizontal burn time for various thrust levels. The green dot represents the baseline case.

seconds is close to achieving the fuel optimal traverse, but there is a fuel savings for thrusting for a shorter period of time with the 100 N engines. The weaker thrust sees a higher minimum fuel at a longer burn time.

Figure 3-3 changes the dependent variable on the y-axis to total traverse time. Also as was seen in Chapter 2, the minimums of these curves occur at their ends; thrusting horizontally for the entire traverse and not coasting at all is the only way to minimize the flight duration. Note that although the baseline traverse minimized fuel consumed with its thrust time, it does not minimize the duration of the traverse. Recall why this is: the minimum traverse time does not correspond to the minimum fuel usage. Yet if time is the driving metric, the fuel cost over the minimum fuel is only 0.20 kg. This could be deemed worthwhile tradeoff.

Another design metric is seen in figure 3-4. This plot has maximum traverse velocity on the y-axis. This velocity increases with burn time and maximum thrust.
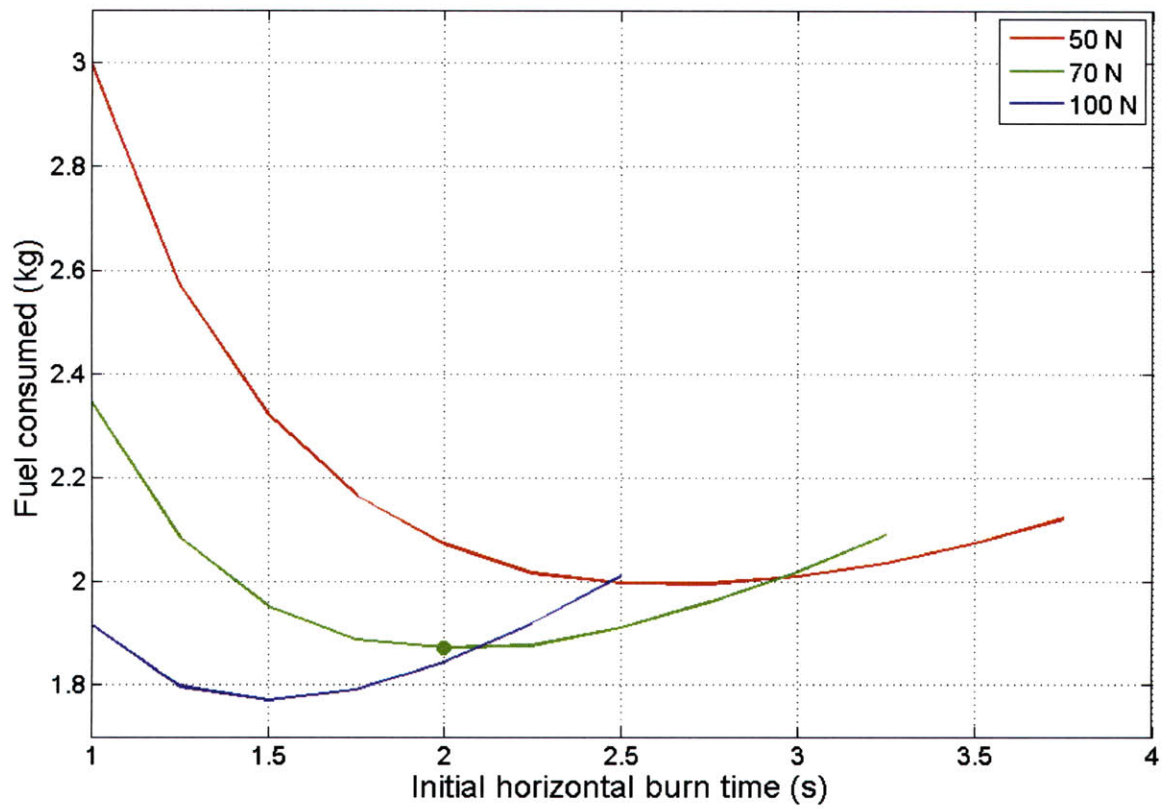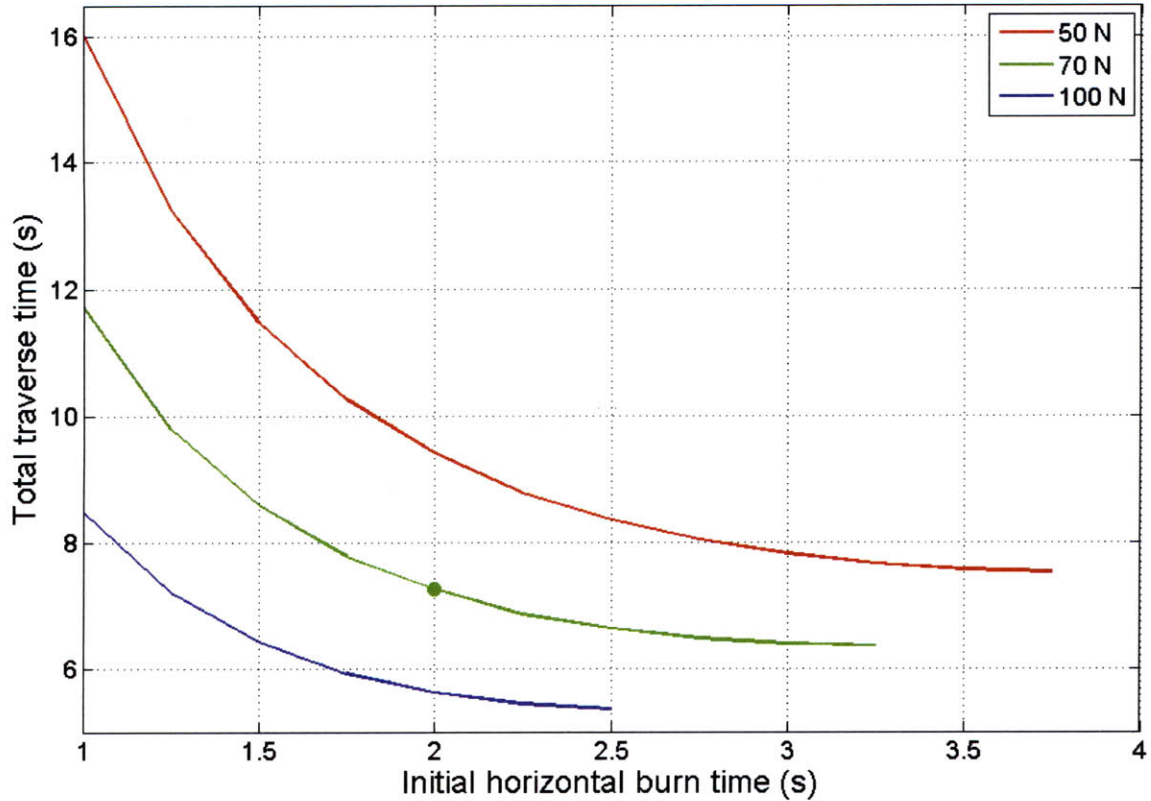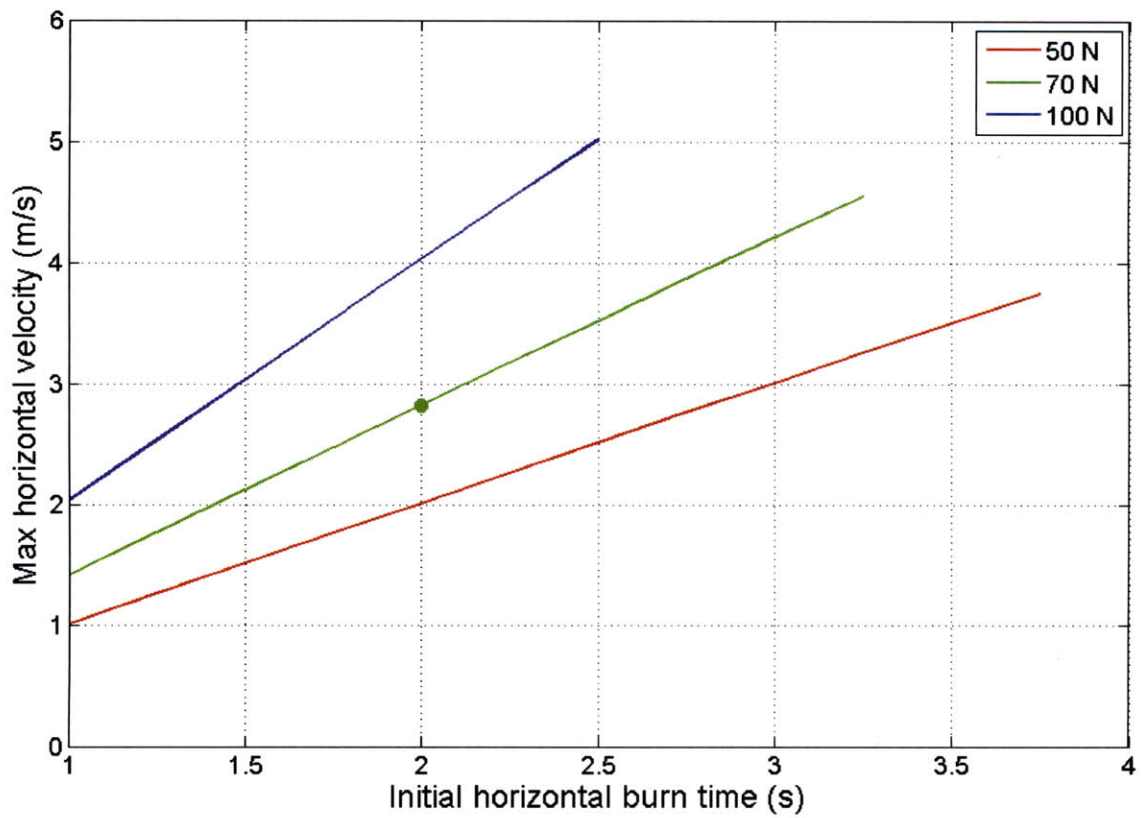
Figure 3-4: Maximum traverse velocity as a function of initial horizontal burn time for various thrust levels. The green dot represents the baseline case.
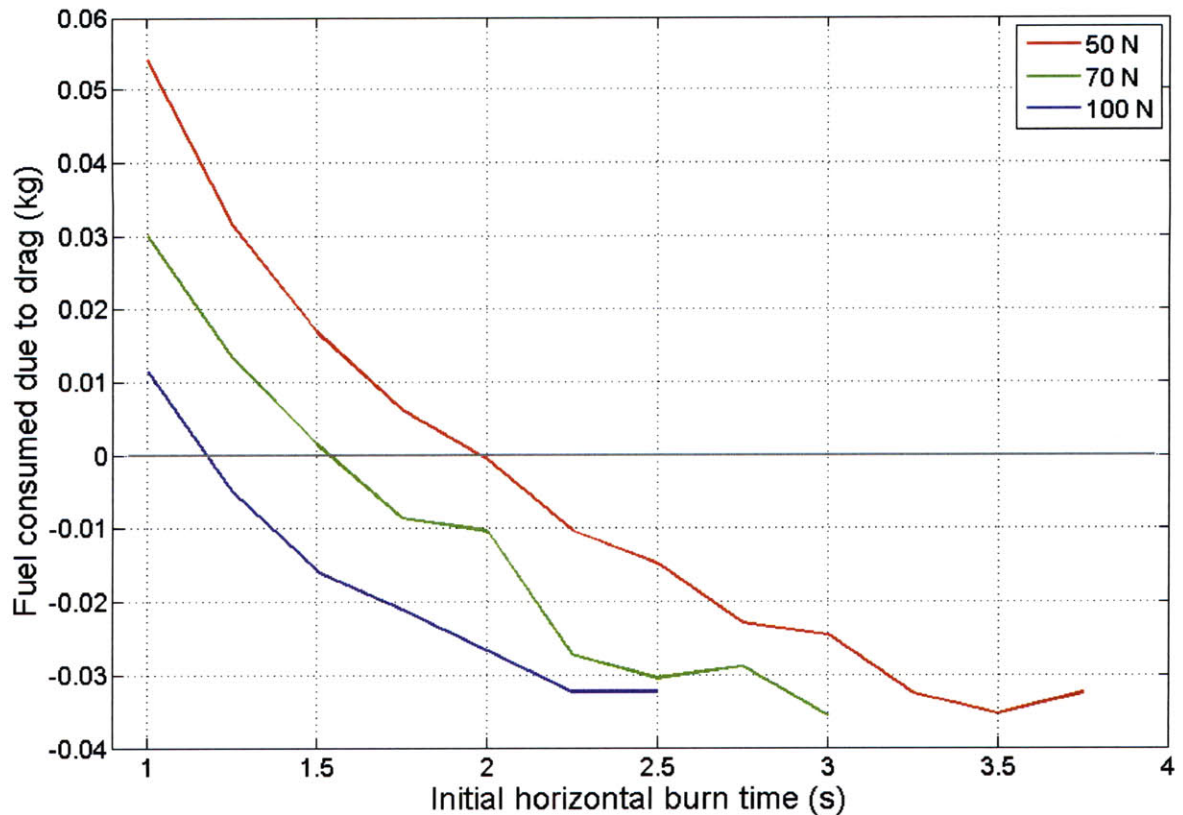
Figure 3-5: Fuel consumed due to drag as a function of initial horizontal burn time for various thrust levels

This data could introduce more constraints if it is determined that the TALARIS structure cannot handle certain speeds, or if the vehicle's maximum allowed velocity is set at a certain value as a safety precaution.

Effects of Drag

Drag will certainly be a factor on Earth, but the question is on its level of significance. The constant distance tradespace was run again, but this time without drag. The data was gathered and differenced from that of the previous instances in order to generate the figures 3-5 through 3-7.

Figure 3-5 shows the fuel consumed due to the Earth's atmospheric drag. These additions are fractions of percents of the overall fuel costs seen in figure 3-2. Interesting to note is that there is a zero crossing, illustrated by the gray line in the figures. That is, there are combinations of thrust levels and initial burn times at which drag is
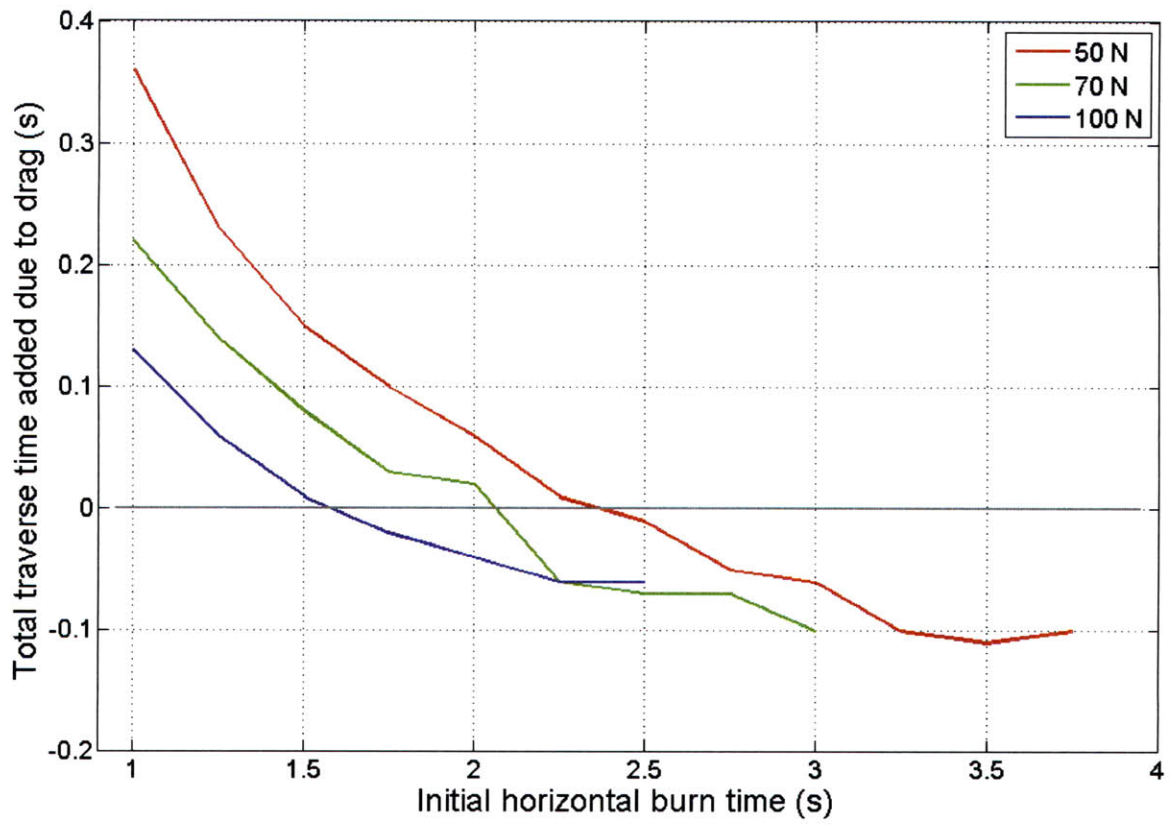
Figure 3-6: Additional traverse time due to drag as a function of initial horizontal burn time for various thrust levels
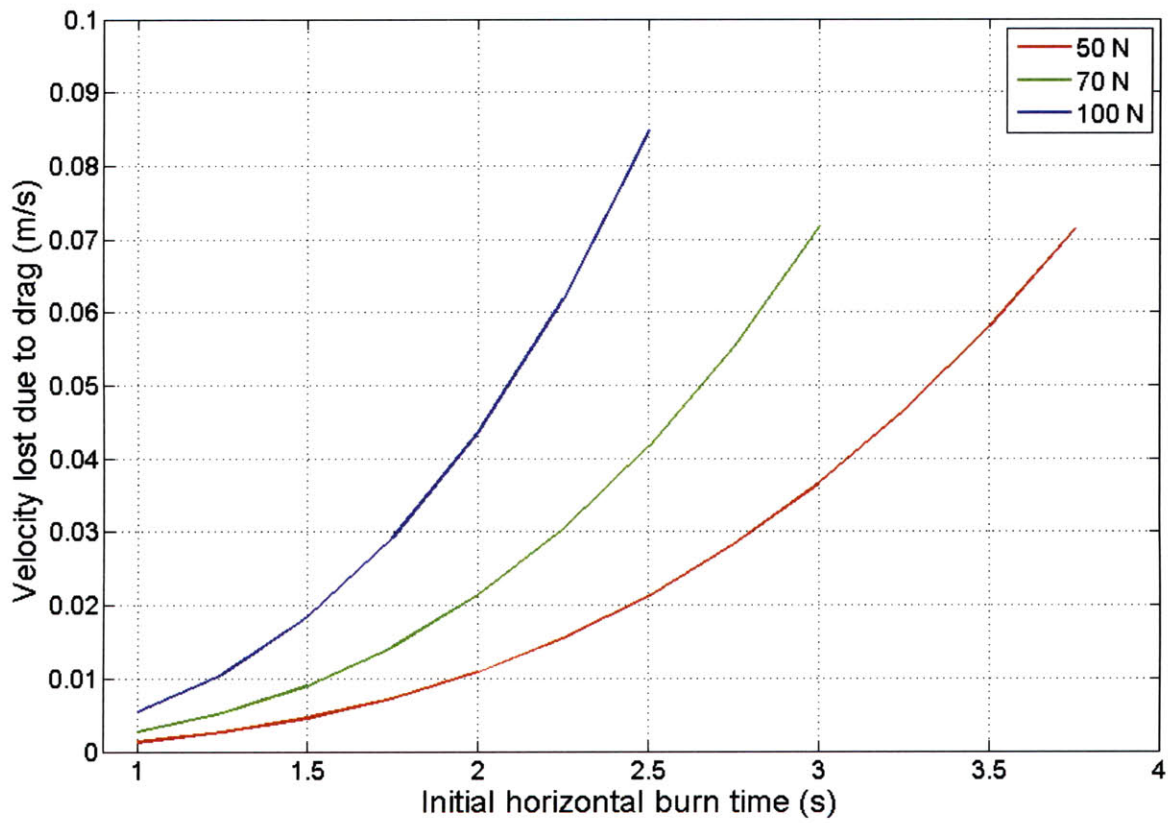
Figure 3-7: Maximum velocity lost due to drag as a function of initial horizontal burn time for various thrust levels

not a factor. Beyond this point, drag actually *saves* fuel; this is because it begins to aid in the vehicle slowdown more than it detracts from the powered traverse. A similar pattern is seen in figure 3-6 with the traverse times. Notice that for the baseline 70 N, 2-second initial burn case, drag results in a slight fuel savings.

Figure 3-7 is a way to examine the energy lost due to drag. It is a plot of the maximum velocity lost, where the maximum velocity is that at the end of the powered traverse. It is seen that for a given burn time, more velocity is lost for the stronger engines. However, at worst case this loss is no more than 0.09 m/s.

Thus, it can be concluded that with the thrust levels currently achievable with TALARIS for the baseline hop, the role of drag will be almost negligible. Nevertheless, as the trends imply, it could become a larger factor if the Earth hopper is given more powerful engines and reaches higher velocities.

3.4   Summary

In this chapter, the Hop Tradespace Tool was modified and used to perform a first-order analysis on the planned TALARIS hover hop demonstration. It was determined that the original baseline hop was not feasible, and for this reason, a new baseline was designed. A parametric study was then done on this new traverse; from this analysis, constant distance and constant thrust time trends were discovered. The effects of aerodynamic drag were also examined and deemed to be present yet small.

Nevertheless, these results only capture the first-order performance of TALARIS by itself. If the Earth hopper is meant to be a testbed for lunar software, it is necessary to investigate how well it emulates what is expected to be seen on the Moon. In other words, there needs to be a performance comparison of TALARIS to the NGL hopper in order to ultimately evaluate its ability to replicate a lunar hop. This final study will be the focus of the next chapter.

Chapter 4

TALARIS and NGL Performance Comparison

The previous chapter was concerned with finding a traverse within the capabilities of TALARIS which will demonstrate a hop. Yet the ability of the Earth hopper to simply perform a hover hop, even while running lunar GN&C software, is only a part of the task. As a prototype for the lunar NGL vehicle, TALARIS is expected to behave as a similar vehicle would on the Moon. If this does not happen then it fails at its purpose. The goal of this chapter is to describe the development of a 3-DOF hopper simulation tool and the analysis run with it in order to show how TALARIS compares to its lunar counterpart.

4.1   Experimental Rationale

If TALARIS could be run on Earth in a low-gravity, vacuum-like environment with a hydrazine propulsion system, there would be little reason to suspect that the hop observed wouldn't be close to that seen on the Moon [1]. However, TALARIS is not afforded these luxuries. Earth and the hopper's hardware introduce a number of factors that won't be seen on the Moon, such as drag and torques caused by

---

[1] This is "close" with respect to energy required, acceleration profiles, and trajectory shape, for example.

asymmetries in EDF thrust. This list is slightly different in 3-DOF, however, and the following are descriptions of these factors in order of potential significance.

EDF Uncertainties

The EDFs are expected to be the largest contributors to any deviations of TALARIS from a nominal lunar mission. If the fans were perfect and always produced thrust equal to 5/6 of the vehicle's weight then there would not be any problems. Yet this will not be the case, primarily because of the sources of error and uncertainty within this system. They can be generalized as:

- **Noise.** The EDFs are electric and as such its control signals will be affected by Gaussian white noise. This will cause the thrust output of the fans to vary with time.

- **Bias**. There may be a bias in the RPM, and thus thrust output, of the EDFs. In other words, the fans may always output a certain RPM above or below what is commanded.

- **Scale factor**. The scale factor here could come from a variety of places, with the most notable being variations in air density as the fans run. If the air density is affected by EDF RPM, there could be reduction in thrust proportional to this value.

These non-lunar, EDF-induced disturbances will result in an off-nominal thrust output, which means TALARIS will appear to go through periods of feeling a gravitational field that is either stronger or weaker than that on the Moon. Furthermore, the EDFs have their own dynamics, which means that corrections won't happen instantaneously. It is unknown how significant the combined effects of these factors will be on the accurate emulation of a lunar hop.

Cold Gas Disturbance Rejection

Both the Earth and lunar thrusters are going to be affected by noise, so in general these uncertainties are not unique to TALARIS. The specific element of the CGS

74

thrusters which could lead to earth-only errors is the disturbance rejection component. This is not a separate system, but rather just refers to how the CGS will be responsible for providing the necessary thrust should the EDFs falter. The uncertainty in these jets will affect how well it can compensate for EDF shortcomings, and their dynamics will control the speed of response. Again, this will impact the gravity felt by the lunar software.

Cold Gas Isp

The physics of the cold gas thrusters results in a propulsion system which has a specific impulse that is a function of the remaining mass in the tanks. Propulsive efficiency sharply decreases after about 2.0 kg are left, meaning fuel will be consumed faster. This relationship is seen in figure 4-1 [2]. Aside from simply using more fuel, the rate at which mass depletes will affect how quickly the EDFs have to respond, again having implications on the simulated gravitational field. Since the lunar hopper will have engines with constant Isp and no EDFs, it's necessary to look into how this effect impacts the elements of the Earth trajectory.

Atmospheric Drag

In Chapter 3 it was shown that drag due to Earth's atmosphere has a relatively minor effect on the vehicle's flight. Nevertheless, it is still a disturbance which is not present on the Moon.

$$* \ * \ *$$

The uncertainty and errors on the EDFs and CGS, the mass-dependent nature of the CGS Isp, and drag are factors which will affect TALARIS but not its lunar counterpart. In order to evaluate the ability of TALARIS to emulate a lunar hopper, it is necessary to see how far these disturbances push its performance away from that which would be seen on the Moon. This analysis will be performed with the aid of the simulation described in the next section.

---

[2] Courtesy of Zach Bailey (MIT).

75
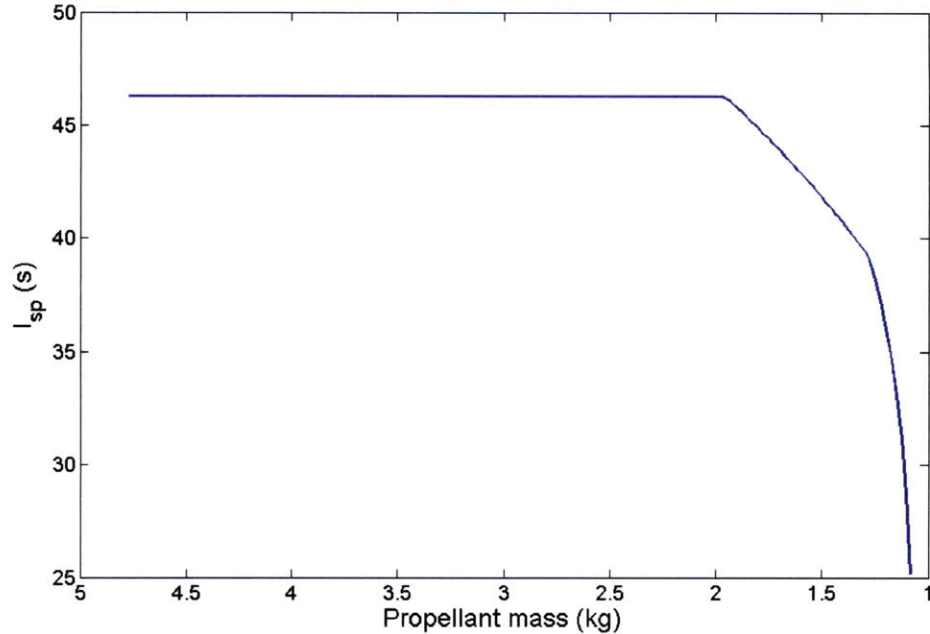
Figure 4-1: Isp as a function of fuel mass remaining

4.2 HopperSim

To perform the comparison between TALARIS and NGL, a simulation tool called HopperSim was developed. HopperSim is a Simulink model capable of performing a 3-DOF hover hop. Although it performs similar calculations as the MATLAB-based HTT, it is more realistic and flexible. Realism comes from a number of features designed to increase the fidelity of the simulated hop, all of which will be described in sections 4.2.1 and 4.2.2. The flexibility is due to the fact that the guidance and control blocks can be updated, there is a placeholder for sensor models, and the whole simulation can be upgraded to support a full six degrees of freedom. HopperSim was designed in this manner such that it could better capture the intricacies of a hopper system.

HopperSim currently contains two main blocks: *Flight Computer* (FC) and *Dynamics*. Their contents and composition were chosen to reflect the actual software and hardware configurations, with a few exceptions. A high-level block diagram is presented in figure 4-2, and the details of the blocks are described next.

76
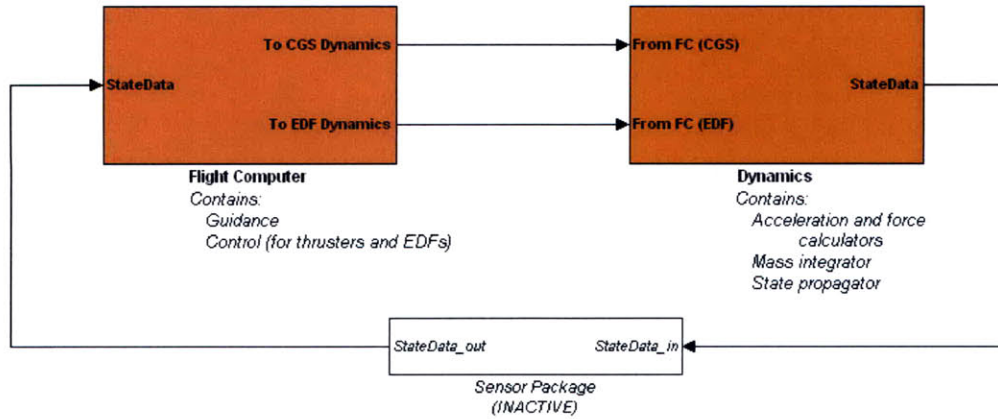
Figure 4-2: HopperSim layout

4.2.1 Flight Computer

Hopper Guidance

Hopper Guidance (HG) is where the state of the vehicle is interpreted to plan and execute the trajectory. It calculates the current $\hat{\mathbf{UP}}$, $\hat{\mathbf{DR}}$, and $\hat{\mathbf{CT}}$ unit vectors, passes through the vehicle mass, and, most importantly, determines the hop phase. That is, based on the hopper's state, HG decides whether the vehicle should be performing its ascent, powered traverse, coast, brake, or descent. This entire package of data is sent to the control blocks.

Thruster Control

The Thruster Control (TC) sub-block uses all outputs from HG in order to send commands to the "actuators". It contains a closed-loop altitude PID controller for altitude. This is responsible for getting the vehicle to the hover height, maintaining its altitude for the hop, and then bringing it back to the ground when commanded. The controller sends out a command at 10 Hz in the form of a percent of the maximum thrust. For traverse control, the TC block adds a multiplier to the $\hat{\mathbf{DR}}$ unit vector depending on the hop phase. This multiplier is 0 for the ascent, 1 for the powered traverse, 0 for the coast, -1 for the brake and 0 for the descent; these will come into play in the Dynamics block. TC also passes through the mass and $\hat{\mathbf{UP}}$.

Note that since this block is responsible for altitude control, its Earth version will be that which performs EDF disturbance rejection. If the EDFs over- or under-work, it is this signal that will differ from that of the lunar hopper.

EDF Control

Whereas the previous subblocks were concerned with controlling the lunar and lunar emulation actuators, the EDF Control (EC) block is the only element of the FC which deals with the Earth-only fans. EC takes in mass and $\hat{\textbf{UP}}$ from HG, and also recieves EDF thrust feedback from the StateData package sent from Dynamics. The purpose of this block is to command and maintain a thrust equal to 5/6 of the hopper's current weight; this is done with the aid of a PI controller. This command, mass, and $\hat{\textbf{UP}}$ are sent to Dynamics.

There are a few idealizations present in the EC block. The first is that with the actual TALARIS, the EDF control software more directly commands an RPM instead of a thrust. However, since the relationship between RPM and thrust proved difficult to capture, thrust was used in the simulation with placeholders present to make the switch when necessary. The second idealization comes from the feedback on mass. TALARIS will not have sensors capable of doing this, so producing a thrust equal to 5/6 of the vehicle's weight (or rather, commanding an RPM which will produce that thrust) is no trivial task. In reality the mass flow rate of the propulsion tanks will be characterized, and a lookup table will be provided to the software telling it when its RPM needs to be changed throughout the mission. For the sake of simplicity of the simulation, this effect is captured by the direct sensing of mass by a fictitious sensor.

4.2.2 Dynamics

The outputs from the FC are all used in Dynamics. The sub-blocks of Dynamics all model the vehicle's actuators and atmospheric effects, when applicable.

Constants

Vehicle Parameters and Planet Parameters contain constants and initial conditions related to the hopper and body it is on, respectively. Initial mass values, aerodynamic properties of the vehicle, the constant thruster Isp, and the maximum traverse thrust reside in the Vehicle Parameters block. In Planet Parameters are the planet's gravitational parameter, radius, and air density.

Thuster Acceleration and Forces Calculator

The Thruster Acceleration and Forces Calculator (TAF) is responsible for producing the vehicle accelerations related to the thrusters. Its inputs are the thruster package from the FC, the maximum thrust and aerodynamic properties from the Vehicle Parameters, air density from Planet Parameters, and velocity from the State Propagator.

To create the acceleration produced by the horizontal thrusters, the traverse thrust is first converted into a percent of total thrust and passed through the Horizontal Jets block. This contains a saturation, pulse creator, time delay, and uncertainty model. The saturation is to ensure that the thrust command does not exceed 100% and does not drop below 0%. The pulse creator turns the command into a sequence of pulses of varying widths, which represents the pulsing that the thrusters will go through to generate thrust. The time delay introduces thruster dynamics into the system, and the uncertainty model contains the elements described in section 4.1 and will be covered more fully in section 4.3. This output is then converted back into a thrust value, divided by the current mass, and then multipled by $\hat{\mathbf{DR}}$. This results in the horizontal acceleration $\vec{\mathbf{a}}_H$.

Obtaining the acceleration produced by the vertical thrusters follows a similar process. The percent commands from the FC are summed from both the lunar and disturbance rejection components. This command is then passed through the Vertical Jets block, which also contains a saturation, pulse creator, time delay, and uncertainty model. This value is then converted to thrust, divided by the current mass, and

multipled by $\hat{\mathbf{UP}}$ to obtain the vertical acceleration $\vec{\mathbf{a}}_V$.

The engine acceleration components $\vec{\mathbf{a}}_H$ and $\vec{\mathbf{a}}_V$ are gathered with the current mass and sent to the Mass Integrator. However, they are not necessarily ready to be passed to the State Propagator in this form. In the instances in which the planet has an atmosphere, the acceleration due to drag is combined with the overall engine acceleration. Drag is calculated using rho, the velocity, c_d, and the area of the appropriate face of the vehicle (its top for vertical drag and its front for traverse drag). These values are divided by mass and the subtracted from $\vec{\mathbf{a}}_H$ and $\vec{\mathbf{a}}_V$ to produce the effective accelerations $\vec{\mathbf{a}}_{H_{eff}}$ and $\vec{\mathbf{a}}_{V_{eff}}$. These are summed as vectors and sent to the State Propagator.

EDF Acceleration and Forces Calculator

The EDF Acceleration and Forces Calculator (EAF) performs the same function as the TAF but for the EDFs. Its inputs are all supplied from the EDF-centric FC commands. The thrust command is first passed through a motor model, which is an experimentally verified time-delay followed by an uncertainty block. This thust output is divided by the mass and then muliplied by $\hat{\mathbf{UP}}$, resulting in the EDF acceleration $\vec{\mathbf{a}}_{EDF}$.

Mass Integrator

The Mass Integrator begins by converting the magnitudes of the thruster accelerations to forces. These forces, along with the thruster Isp, are used to calculate the mass flow rate, $\dot{m}$.

Ideally, Isp would stay essentially constant over the duration of a hop. However, this is not the case with TALARIS and as such the capability to handle a varying Isp was implemented in HopperSim. For the lunar hopper, a flag in the initialization script controls a switch which tells the simulation to use the constant Isp from Vehicle Parameters. In the TALARIS case, the flag causes the switch to use the other input, which accesses the TALARIS Dynamic Isp block. Inside this block is a lookup table which uses preloaded vectors of thuster specific impulse and mass (experimentally

obtained) to output the appropriate Isp based on the fuel mass remaining.

With the forces and specific impulse, $\dot{m}$ can be calculated. Then, along with the initial mass supplied from Vehicle Parameters, $\dot{m}$ is integrated in time to produce the current mass of the hopper. This is placed into the package called StateData.

State Propagator

The State Propagator is a Simulink version of the Runge-Kutta integrator used in the HTT. It uses the engine accelerations from the Forces Calculator, planet data from the Planet Parameters sub-block, and initial state conditions from the initialization script to move the vehicle forward in time. The outputs are position, velocity, and net acceleration. Along with the new mass, these values are packaged into StateData and sent to the FC for the next timestep.

4.2.3 Other Blocks

Two more major blocks exist in the simulation. *To Workspace* is where all relevant parameters are collected in order to be analyzed in the MATLAB workspace. *Stop Conditions* contains the triggers which stop the simulation. Although they can be configued freely, the defaults are 1) when the altitude drops below zero meters, and 2) when the usuable fuel mass reaches zero.

4.3 Procedures

4.3.1 Implementation of uncertainty

The primary goal of this study is to investigate the effects of the Earth-only factors outlined in section 4.1 on the ability of TALARIS to emulate a lunar hop. Section 4.2.2 explained how both the mass dependant Isp and drag force are factored into HopperSim. Now it is appropriate to describe the implementation of the actuator error and uncertainty in detail. As mentioned in section 4.1, errors can enter into a

81
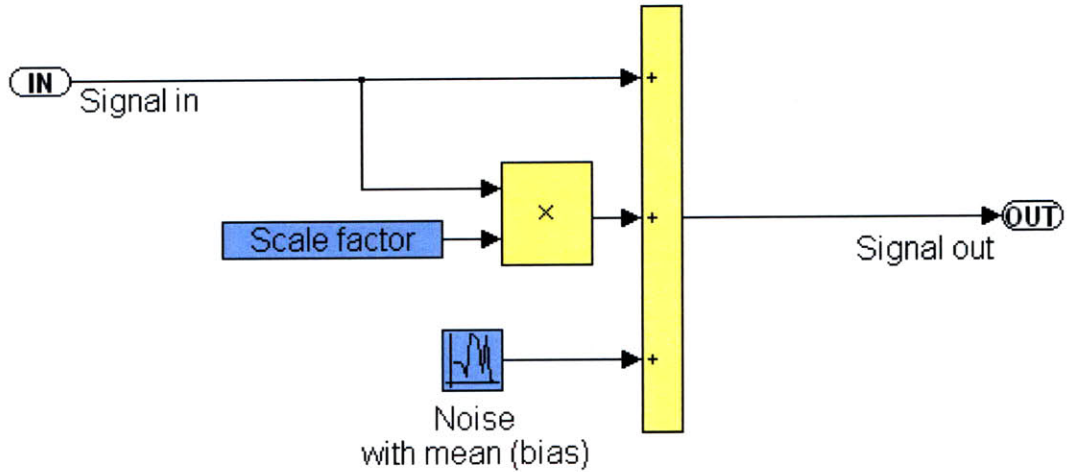
Figure 4-3: Error model. This is the implementation of noise, bias, and scale factor into the HopperSim

signal by means of a bias, noise, or scale factor. The Simulink interpretation is shown in figure 4-3.

As an equation, the output signal can be written as:

$$signal_{out} = signal_{true}(1 + S) + B + N \qquad (4.1)$$

Or, the corrupted output signal is equal to the input signal times the quantity one plus the scale factor, plus the bias and noise. In HopperSim this model is applied to the thrust outputs of the CGS and EDF in their respective actuator blocks. These corrupted thrusts, different from that which was commanded, are used to propagate the state.

4.3.2 Experimental Setup

Three separate but related studies will be performed using HopperSim. They are as follows:

Hover height	2.0 meters
Traverse distance	15.0 meters
Initial downrange thrust time	2.0 seconds

Table 4.1: Parameters of the baseline hop

TALARIS vs. LunarTALARIS

The main analysis is aimed at answering the question posed at the beginning of this chapter. That is: how does a TALARIS hop on Earth relate to what is expected to be seen on the Moon? To do this, HopperSim will be configured to run as TALARIS and a theoretical lunar hopper called LunarTALARIS. LunarTALARIS has the same physical parameters as the Earth hopper with the exception of its Isp being constant [3]. This is done to isolate what is trying to be investigated—the effects of non-Moon factors—from the impacts of physical and hardware differences between the TALARIS and NGL [4].

Given the nature of actuator noise and the possible ranges of biases and scale factors, one simulated hop for each vehicle will not be enough to capture the full space of disturbances which could be experienced. Thus, this study is a perfect candidate for a Monte Carlo analysis. The Monte Carlo process will produce a spread of data which can then be statistically analyzed in order to get a feel for the effects of disturbances on the trajectory, including how far they cause deviations from the nominal lunar hop. One-thousand Monte Carlo runs will be performed for the both the Earth and lunar baseline hops. The baseline hop will be the same examined in Chapter 3; the parameters are re-listed in table 4.1.

Parametric study of actuator uncertainty

Although the error values on the EDFs and thrusters were obtained from tests in the lab, they were extrapolated from the results of other experiments and weren't obtained via specific studies on actuator error. As such, the results from the TALARIS

---

[3] Think of this lunar version being TALARIS with the EDFs serving as payload and with a very low engine efficiency.

[4] Cold gas being used for TALARIS is considered a non-Moon factor

vs. LunarTALARIS analysis may not account for the actual uncertainty present in the EDFs and CGS. This second study will revisit the TALARIS/LunarTALARIS comparison while trying three additional noise variances on the actuators. The goal here will be to see how much error TALARIS can handle before it deviates too far from the profile of a lunar hop.

NGL vs. EarthNGL

Instead of investigating how an Earth prototype would perform in a lunar environment, the final analysis will examine how the lunar vehicle would work on Earth. The scenario assumes that a fully-functional NGL is constructed and needs to be tested. It is connected to EDFs and sent on the baseline hop. The question now becomes: how well can NGL perform with Earth disturbances and the simulated lunar gravity field? This will also give insight on ability of the flight software to work on both vehicles. For this study, HopperSim will be configured to be the NGL hopper, and 1000 Monte Carlo trials will be run for both the lunar and Earth hops.

4.3.3   Process

The three files used are:

1. The *Monte Carlo wrapper* is where the uncertainty values for the EDF and CGS set. It also calls the initialization script and runs the simulation the specified number of times. The wrapper also stores all output data for analysis.

2. The *initialization script* sets all initial conditions and constants for the Simulink model.

3. And finally, the Simulink *HopperSim model* executes the hop.

Statistical data, such as average and standard deviation, will be collected across all 1000 runs for each study. Analysis will be performed related to fuel, mission time, velocities, and general trajectory profiles.

	CGS thrusters	EDFs
Noise (1-σ)	2 %	5 N
Bias (1-σ)	0	1 N

Table 4.2: Uncertainty values for the CGS thrusters and EDFs

	Fuel (kg)	Time (s)	Max traverse velocity (m/s)
MOON - *Entire hop*	3.117	14.73	2.86
Ascent	0.528	3.00	-
Traverse	1.816	7.27	2.86
Descent	0.772	4.46	-

	Fuel (kg)	Time (s)	Max traverse velocity (m/s)
EARTH - *Entire hop*	3.233	15.49	2.84
Ascent	0.529	3.00	-
Traverse	1.837	7.26	2.84
Descent	0.867	5.23	-

Table 4.3: Nominal trajectory results

4.4 Results

4.4.1 TALARIS vs. LunarTALARIS

4.4.1.1 Uncertainty parameters

The uncertainty values on the actuators are seen in table 4.2. These values were selected based on tests performed with the EDFs and CGS which are outside the scope of this thesis; note that scale factors were not used since they were not studied in any depth. The bias was then multiplied by a normally distributed random number for each trial. For a more in-depth explanation of the data used, see the appendix.

4.4.1.2 Nominal and control trajectories

The nominal trajectories come from simulating an Earth and lunar hop without adding any uncertainty to the actuators. Table 4.3 shows data for these hops, while figures 4-4 through 4-6 show their trajectories and position and velocity profiles. A description of these profiles is as follows. From t = 0 to t = 5, both hoppers remain stationary; for TALARIS the EDFs are ramping up to 5/6 of its weight. The vertical thrusters turn on at t = 5 and the vehicles begin their ascent. This is seen in
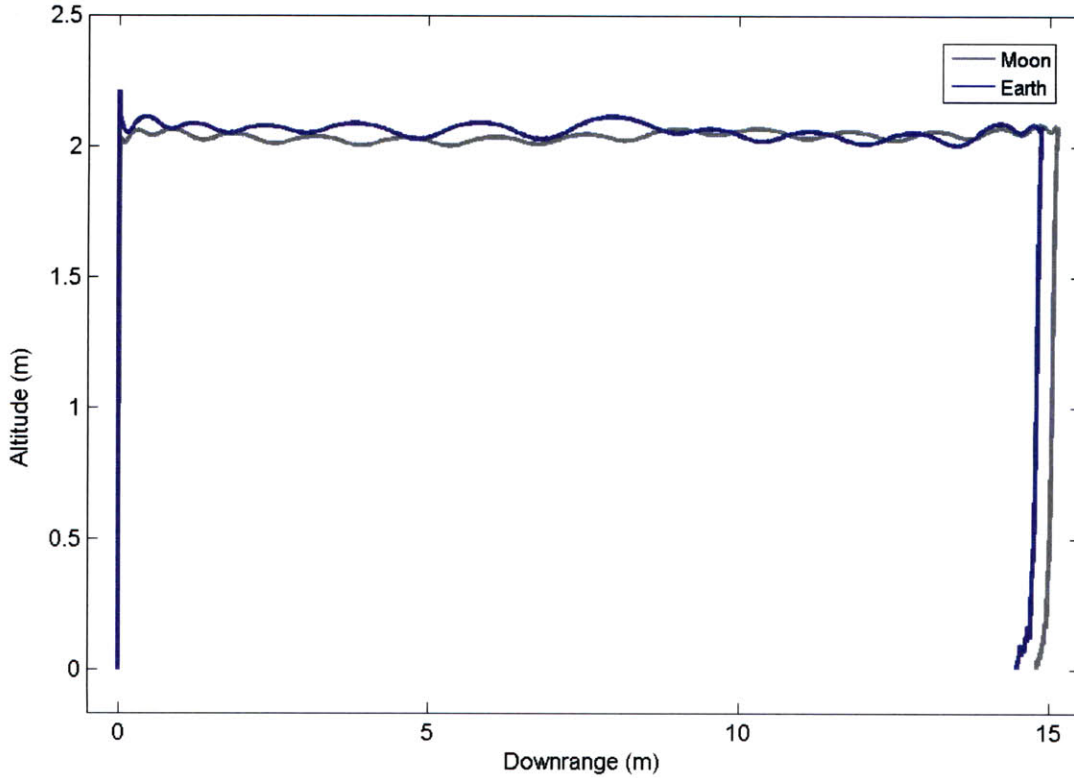
Figure 4-4: Trajectory shape of nominal Earth and lunar hops

the increase in altitude and change in vertical velocity. The vertical velocity profile shows that the PID controller initially commands a high thrust before it backs down, while the altitude profiles illustrate the vehicles reaching the 2.0-m target height and settling around it.

At t = 8 the powered traverse begins; notice how the downrange positions and velocities begin to increase. Also during this traverse, due to the pulsing of the vertical thrusters, there are slight oscillations in the vertical velocities and positions. This phase lasts for two seconds, and at t = 10 the horizontal thrusters turn off and the coast starts. Note how the horizontal velocity stays constant during the lunar hop, but is actually reduced during the Earth hop due to the presence of drag.

The braking phase begins around t = 13.5. The horizontal thrusters oppose the hoppers' motions in order to bring the traverse velocity to zero. As expected, the plots show a sharp decrease in horizontal velocity. Finally, around t = 15, the hoppers reach the desired downrange position. The horizontal thrusters turn off
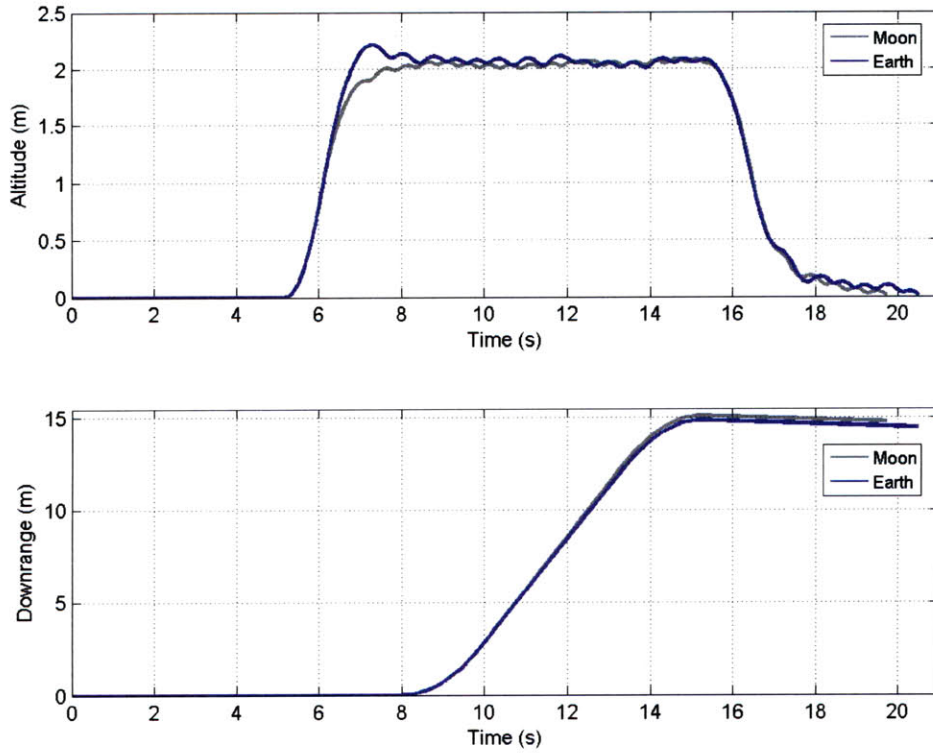
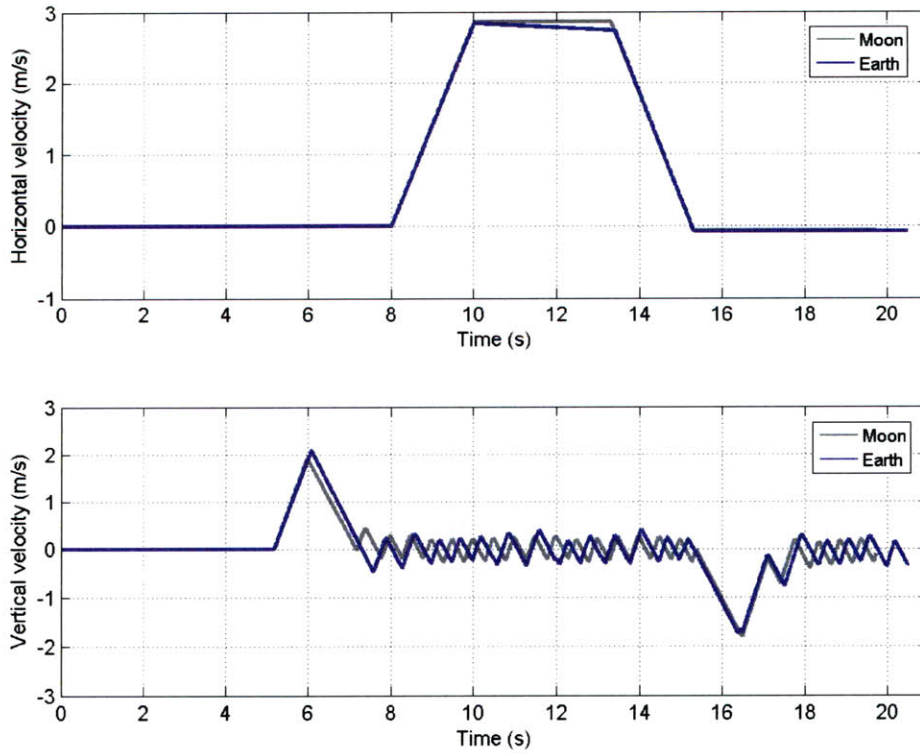Figure 4-5: Position profiles of nominal Earth and lunar hops

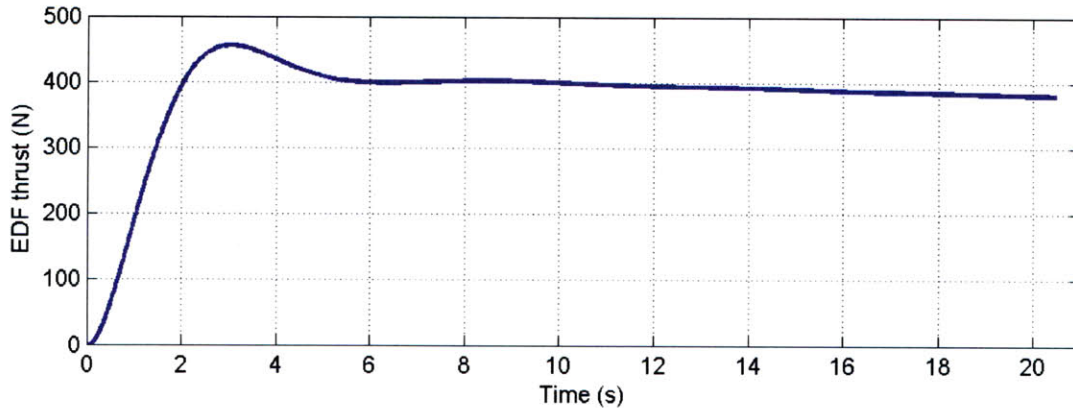Figure 4-6: Velocity profiles of nominal Earth and lunar hops

Figure 4-7: EDF thrust profile over time

and the PID controller commands the vertical thrusters to bring the vehicles to the ground. The profiles show that the horizontal velocities are now zero as the vertical velocities become negative due to the descent. The movement is reflected in the position profiles.

Unique to TALARIS are its EDFs. Figure 4-7 shows the nominal EDF thrust over time. As mentioned above, the fan system ramps up to the proper thrust for the first five seconds. Afterward it adjusts its throttle in an effort to maintain a thrust equal to 5/6 of the hopper's current weight. This value is roughly 400 newtons.

The nominal trajectories are just one form of experimental control. They provide intuition on how the hopper is supposed to perform, and they can also be used as benchmarks to evaluate how far disturbances take the hoppers away from the ideal operation. Yet there is another control trajectory. Since LunarTALARIS will also have disturbances on its actuators, comparing Monte Carlo runs of TALARIS to the nominal lunar hop data would not be accurate. Thus, 1000 Monte Carlo trials will be carried out for the lunar hop as well, and this will be the Moon hop to which the Earth hops will be compared. Table 4.4 shows its parameters, figure 4-8 shows the average trajectory, and figure 4-9 shows its velocity profiles.

	Fuel (kg)	Time (s)	Max traverse velocity (m/s)
Entire hop	3.199	15.28	2.87
Ascent	0.523	3.00	-
Traverse	1.849	7.27	2.87
Descent	0.827	7.69	-

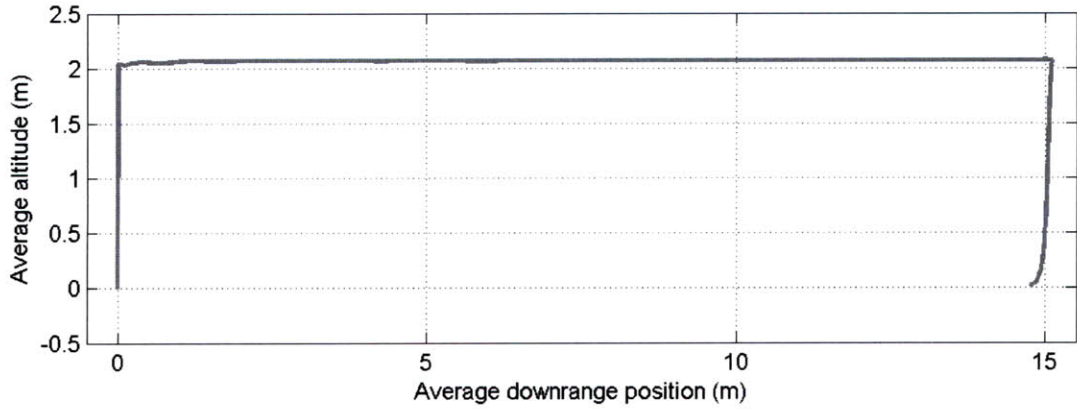Table 4.4: Average results for 1000 lunar hops with disturbances
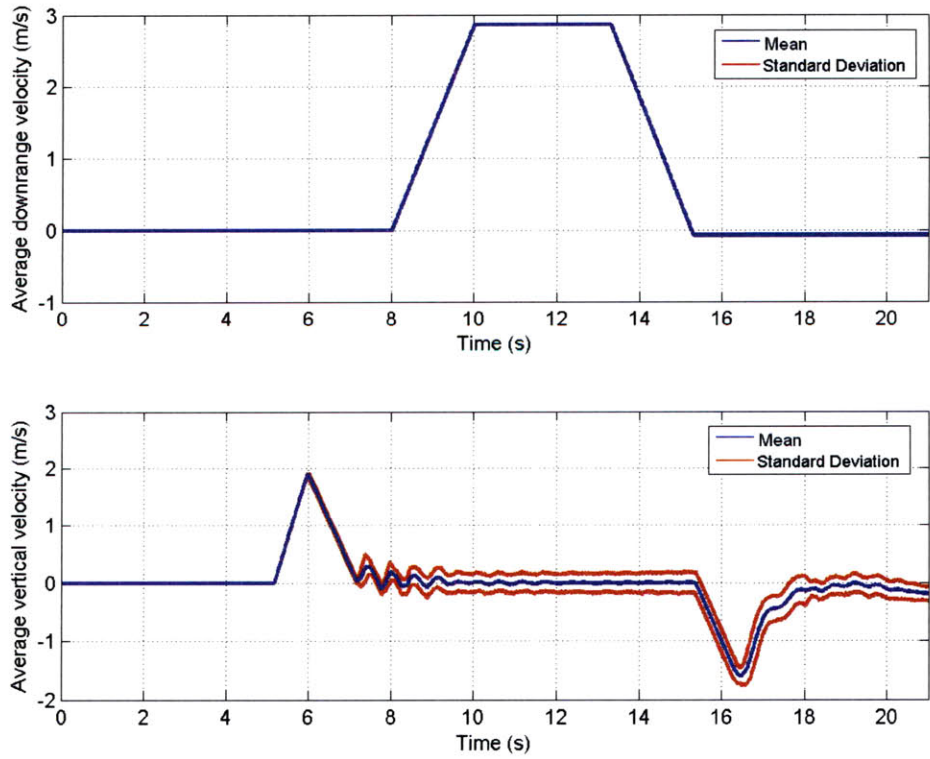

Figure 4-8: Average lunar hop

Figure 4-9: Average velocity for a lunar hop

89

	Fuel (kg)	Time (s)	Max traverse velocity (m/s)
Average	3.171	15.07	2.84
Standard deviation	0.127	0.69	1.14×10^{-4}
Earth Average - Nominal Earth	-0.062	-0.42	0
Earth Average - Lunar Average	-0.028	-0.21	-0.03

Table 4.5: Earth hop statistics

4.4.1.3 Monte Carlo analysis - Full Hop

All hops

An overview of a full set of Earth hops can be described with the data in table 4.5. The first two rows show statistics for this hop, whereas the second two show the differences between those statistics and that of the control trajectories. Figure 4-10 shows histograms for all Monte Carlo runs. Figure 4-11 is a plot of its average trajectory, and figure 4-12 contains its velocity profiles.

In table 4.5, it is seen that the average TALARIS hop is slightly cheaper than both the nominal and lunar versions. It requires a 2% decrease in fuel from the nominal Earth hop, and a 0.9% decrease from the average lunar hop. Furthermore, the Earth hop, on average, takes under half a second less to perform its maneuver. There is only a decrease in maximum velocity from the average lunar case. Thus, from this data, it appears as if the introduction of disturbances does not draw TALARIS far from its nominal course or its counterpart on the Moon.

Successful hops only

Due to uncertainties on the actuators, there is a possibility that certain hops will fail. A failed hop satisfies at least one of the following criteria:

- The vehicle runs out of fuel before the trajectory is completed

- The vehicle hits the surface before 14-meters

- The vehicle's altitude exceeds 3.0 meters at any point along its trajectory

The first two points are straightforward: the mission must be aborted if the fuel is depleted prematurely, and the mission is a failure if the hop ends too early. The
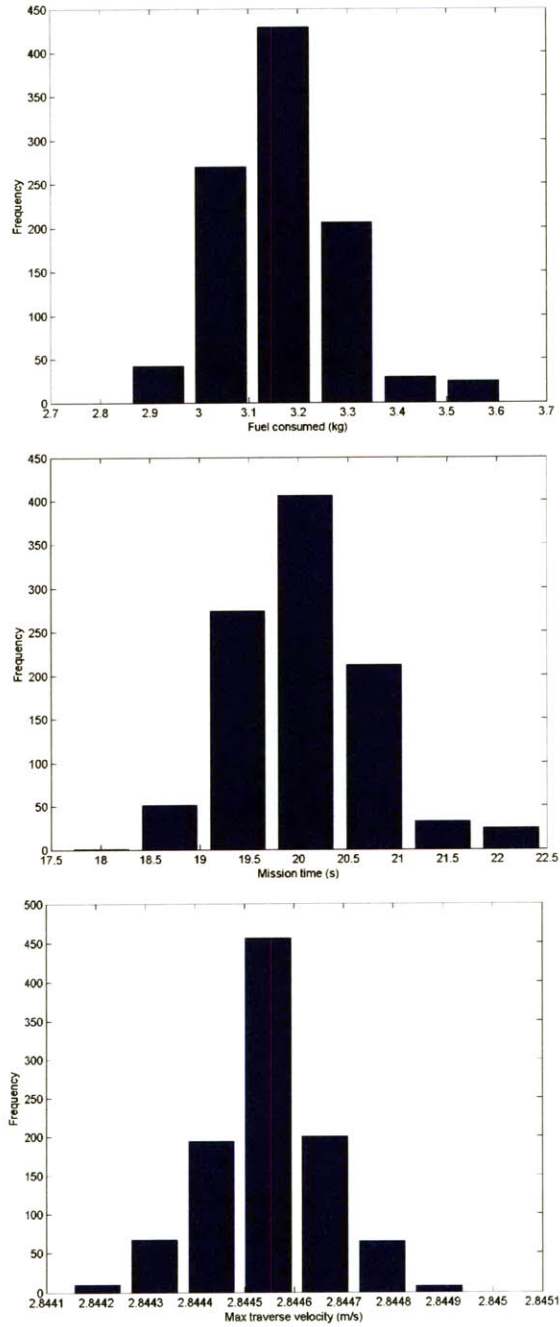
90

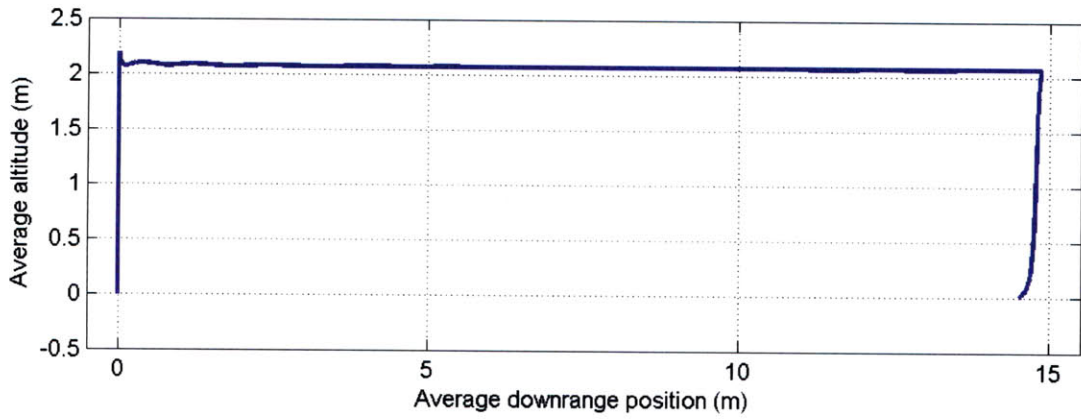Figure 4-10: Results of Monte Carlo runs for an Earth Hop
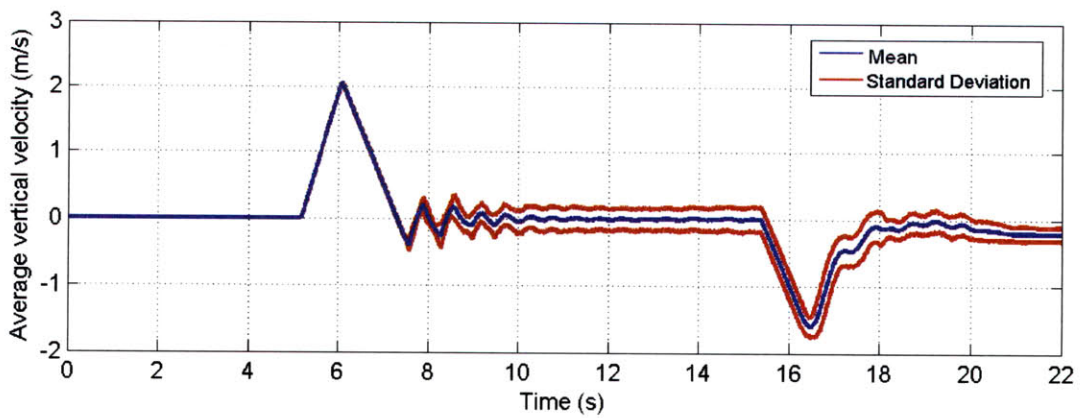
Figure 4-11: Average Earth hop
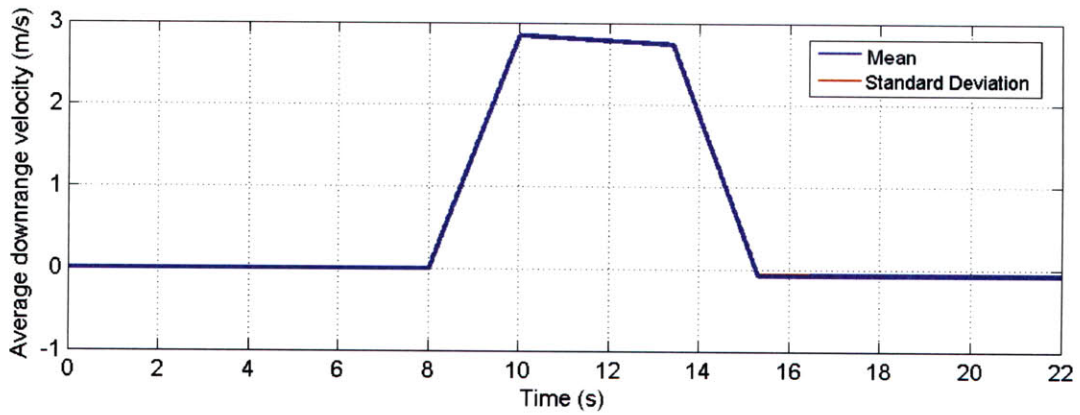
Figure 4-12: Average Earth hop velocities

	Fuel (kg)	Time (s)	Max traverse velocity (m/s)
Average	3.163	15.04	2.84
Standard deviation	0.112	0.63	1.15×10^{-4}
Earth Average - Nominal Earth	-0.070	-0.45	0
Earth Average - Lunar Average	-0.036	-0.24	-0.03

Table 4.6: Earth hop statistics (Successful hops)

altitude criteria is somewhat arbitrary; however, it can be assumed that if the hopper flies too far above its target hover height than it is likely to go unstable. Furthermore, for practical purposes, during testing it is important that TALARIS does not fly higher than its test stand.

The Monte Carlo data shows that 17 of the 1000 cases fail. Or in other words, the TALARIS flight was successful over 98% of the time. Otherwise, the trajectories satisfy at least one of the failed hop criteria. Although the failed cases are few, there is still merit in removing them and seeing their effect on the hop statistics. This data is listed in table 4.6.

It is seen that by removing the failed cases, the average TALARIS hop consumes 0.25% less fuel and takes 0.03 seconds longer than before. This change is also reflected in the differences from the control trajectories. Although the difference is slight, it is this data free of the failed hops which will be used for the remainder of the TALARIS vs. LunarTALARIS analysis.

4.4.1.4 Hop by phase

Breaking the trajectory apart by phase can give more insight on the differences between the Earth and lunar hops at their different stages. Table 4.7 lists the statistics for the Earth traverse along with how they compare to that of the nominal and lunar versions.

For the traverse and ascent, the fuel differences are on the order of fractions of percents. The largest gaps between the average Earth hop and the control trajectories are during the descent; here, TALARIS uses about 7% and 3% less fuel than the nominal Earth and lunar cases, and takes almost two seconds more time than nominal

	Fuel (kg)	Time (s)	Max traverse velocity (m/s)
TRAVERSE AVERAGE	1.834	7.26	2.84
Earth Average - Nominal Earth	-0.003	0	0
Earth Average - Lunar Average	-0.015	-0.01	-0.03
ASCENT AVERAGE	0.526	3.00	
Earth Average - Nominal Earth	-0.003	0	
Earth Average - Lunar Average	0.003	0	
DESCENT AVERAGE	0.803	6.98	
Earth Average - Nominal Earth	-0.064	1.75	
Earth Average - Lunar Average	-0.024	-0.71	

Table 4.7: Successful Earth hop statistics by phase

	Set 1 (original)	Set 2	Set 3	Set 4
EDF noise (1-σ)	5 N	10 N	100 N	1000 N
EDF Bias (1-σ)	1 N	1 N	1 N	1 N

Table 4.8: Uncertainty values for the CGS thrusters and EDFs

and under a second less than the Moon hop. Yet overall the parameters of the hops are very similar in nature, implying that, for those cases which do not fail, TALARIS can indeed closely emulate a hop on the Moon.

4.4.2 Actuator Uncertainty Study

Uncertainty parameters

As mentioned in section 4.3.2, the uncertainty values selected for the actuators weren't obtained through direct means. As such, it is possible that they are not accurate. For this reason it makes sense to investigate a range of uncertainty values, specifically noise, in order to get a better picture of the effect on TALARIS. This will also shed light on how much noise can be present in the EDFs before the hop fails. Table 4.8 shows the parameters selected for each experimental set. One-thousand Monte Carlo runs of the Earth hop were performed for each set of parameters.

Full hop analysis

Table 4.9 lists the pertinent results from each trial, with the fuel and altitude data for non-failed cases only.

94

	Failed cases (%)	Av. fuel / std dev	Av. traverse altitude / std dev
Set 1 (Original)	1.7	3.163 / 0.112	2.069 / 0.031
Set 2	2.3	3.163 / 0.112	2.051 / 0.020
Set 3	4.9	3.172 / 0.143	2.062 / 0.025
Set 4	84.4	2.843 / 0.259	2.188 / 0.233

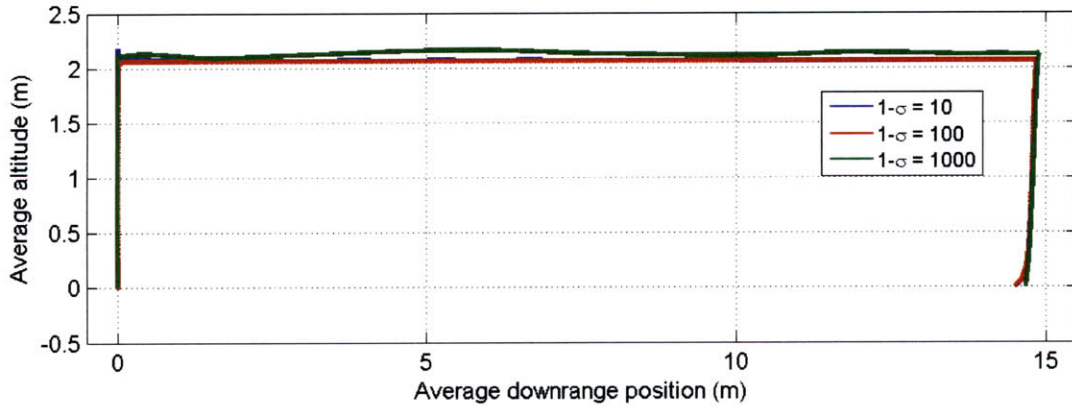Table 4.9: Results of uncertainty parametric study

Figure 4-13: Average trajectories of the Earth hop in all three sets

First to note is the number of failed hops in the first column. For sets #1 through #3, in which the standard deviation of the EDF noise has a range on the order of 10^2, the percent of failed cases remains under 5%. Furthermore, the average fuel required for the hop as well as the average traverse altitude remains close together (within 0.3%). The spreads, as illustrated by the standard deviations, are relatively similar as well.

These trends do not hold with the fourth set. Here, over 80% of the cases fail. The traverse altitude and standard deviations are the highest (despite the average fuel required being less). This is somewhat expected, however, since the standard deviation of the noise in set #4 is significantly greater than the nominal thrust of about 400 newtons required from the EDFs. Figure 4-13 shows the average trajectories of sets #2 through #4; sets #2 and #3 are hardly distinguishable.

Wet mass	112 kg
Dry mass	86 kg
Thruster Isp	230 s
Maximum vertical thrust	440 N (110 N per thruster)
Maximum traverse thrust	44 N (22 N per thruster)

Table 4.10: Projected parameters for the NGL hopper

Remarks

From this analysis, it can be concluded that a TALARIS flight can be successful as long as the standard deviation of the noise on the EDFs remains less than their required thrust output. The third trial used assumed the noise was two orders of magnitude worse than what has been observed in the lab and there was no significant difference between its results and that of sets #1 and #2. However, as set #4 illustrated, having noise that exceeds the thrust of the EDFs is detrimental to the maneuver: a successful hop was completed only about 16% of the time. Thus, although noise on the fans should be kept as low as possible, it can be near the required thrust output without posing an increased threat to the success of the hop.

4.4.3 NGL vs. EarthNGL

4.4.3.1 NGL Parameters

Although the NGL vehicle has not been built yet, table 4.10 lists its projected parameters. The theoretical Earth counterpart to NGL, called EarthNGL, is identical in every way except for the fact that it has EDFs [5]. Also keep in mind that these vehicles are using the same flight software, i.e. guidance and control algorithms, as the TALARIS family.

---

[5]To keep the mass the same, assume that either the EDF system is light in comparison to the rest of the vehicle, or that EarthNGL has mass moved from elsewhere in order to make room for the fans.
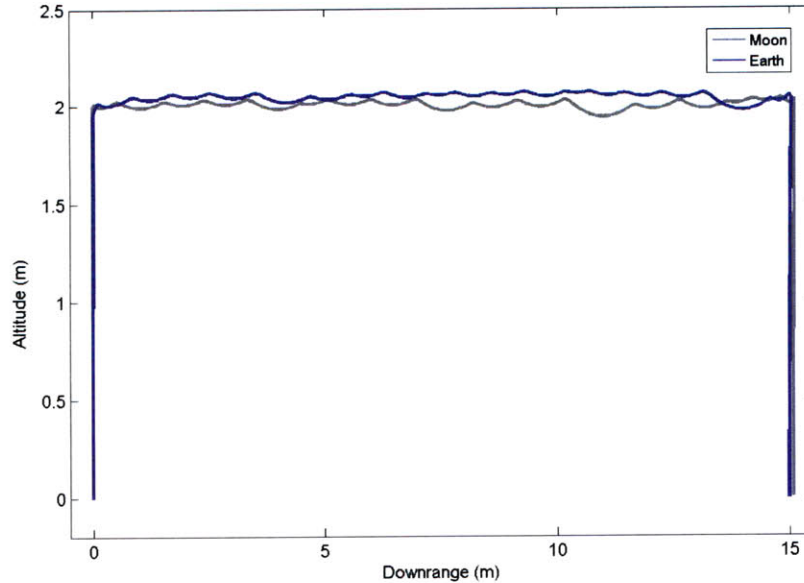
Figure 4-14: Trajectory shapes of nominal Earth and lunar hops

4.4.3.2 Nominal NGL Profiles

Figures 4-14 through 4-16 show various profiles for the nominal hops. As with TA-LARIS, the first five seconds are to allow the EDFs, if present, to ramp up to their necessary RPM. The ascent begins at t = 5, but notice how the ascent and settling takes seven additional seconds–this is over twice as long as TALARIS. The traverse starts at t = 12 and ends around t = 33. Realize that this traverse is longer because the NGL is heavier and has weaker thrusters than TALARIS, resulting in a lower traverse velocity. Finally, the descent brings the hopper back to the surface. For EarthNGL, figure 4-17 shows the thrust provided by the EDFs. Table 4.11 summaries the data presented in the figures.

4.4.3.3 Monte Carlo analyses

Table 4.12 summarizes the average lunar NGL hop, the average Earth NGL hop, and the difference between the Earth maneuver and the two control trajectories. Figure 4-18 shows the average trajectories of the two hops. For the Earth hop the data is for all hops since all 1000 Monte Carlo runs were successful.

EarthNGL, like TALARIS, remains fairly accurate when compared to its lunar
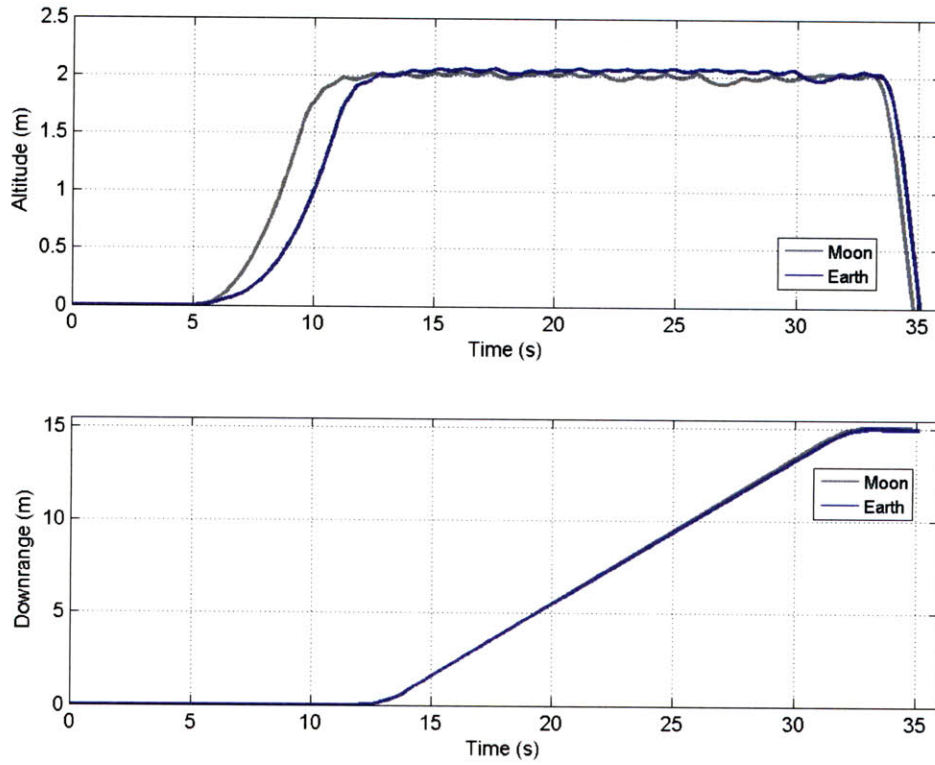
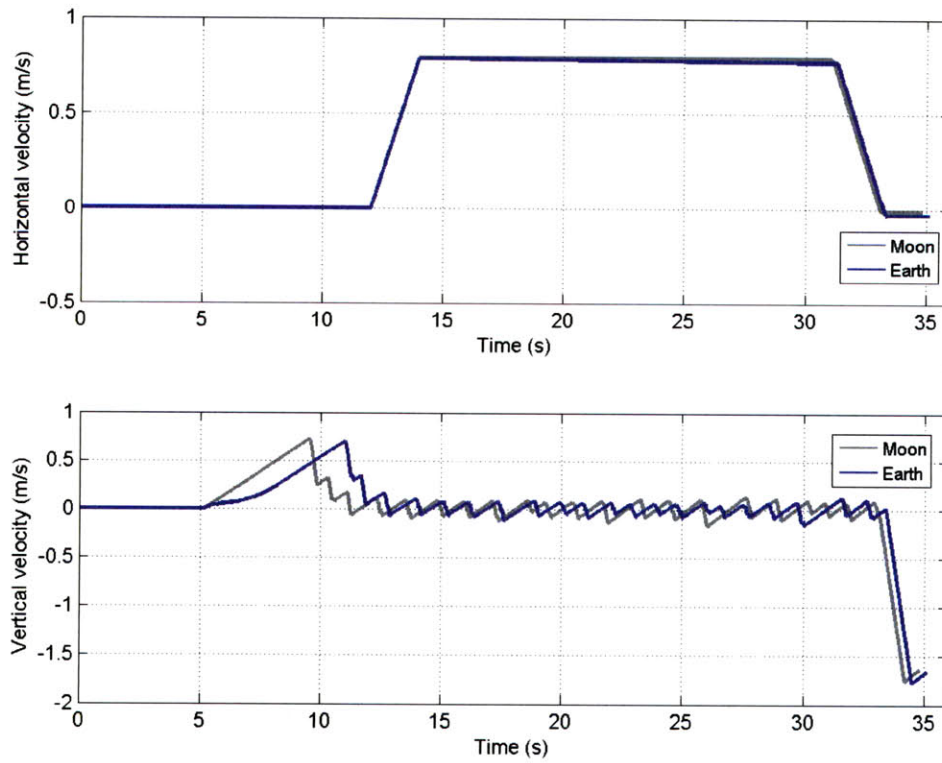Figure 4-15: Position profiles of nominal Earth and lunar hops

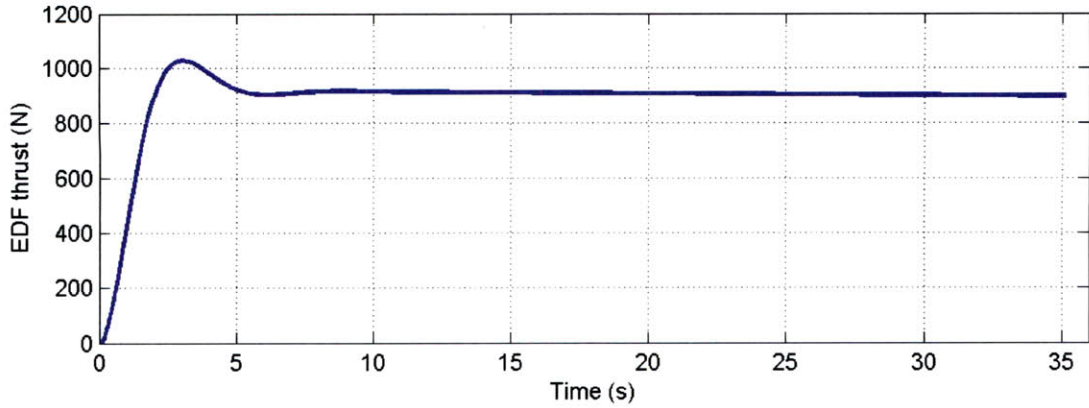Figure 4-16: Velocity profiles of nominal Earth and lunar hops

Figure 4-17: EDF thrust profile over time

	Fuel (kg)	Time (s)	Max traverse velocity (m/s)
MOON - *Entire hop*	2.362	29.83	0.79
Ascent	0.553	7.00	-
Traverse	1.748	21.09	0.79
Descent	0.061	1.74	-
	Fuel (kg)	Time (s)	Max traverse velocity (m/s)
EARTH - *Entire hop*	2.415	30.12	0.79
Ascent	0.568	7.00	-
Traverse	1.777	21.24	0.79
Descent	0.071	1.88	-

Table 4.11: Nominal NGL trajectory results

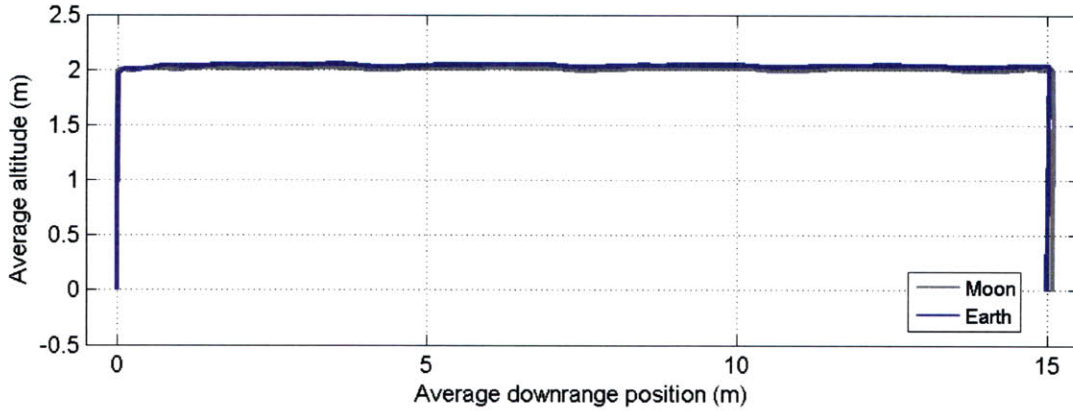|	Fuel (kg)	Time (s)	Max traverse velocity (m/s)
Average NGL hop	2.368	29.90	0.79
Average EarthNGL hop	2.418	30.13	0.79
Standard deviation	0.005	0.04	2.34×10^{-6}
Average Earth - Nominal Earth	0.003	0.01	0
Average Earth - Average lunar	0.050	0.23	0

Table 4.12: Hop statistics for the NGL vehicles

99

Figure 4-18: Trajectory shapes of average Earth and lunar NGL hops

	Fuel (kg)	Time (s)	Max traverse velocity (m/s)
AVERAGE EARTHNGL TRAVERSE	1.776	21.24	0.79
AVERAGE NGL TRAVERSE	1.750	21.09	0.79
Earth Average - Nominal Earth	-0.001	0	0
Earth Average - Lunar Average	0.026	0.15	0
AVERAGE EARTHNGL ASCENT	0.569	7.0	
AVERAGE NGL ASCENT	0.553	7.0	
Earth Average - Nominal Earth	0.001	0	
Earth Average - Lunar Average	0.016	0	
AVERAGE EARTHNGL DESCENT	0.072	1.96	
AVERAGE NGL DESCENT	0.065	1.90	
Earth Average - Nominal Earth	0.001	0.08	
Earth Average - Lunar Average	0.007	0.06	

Table 4.13: NGL hop statistics by phase

version. Thus we can conclude that during successful hops an Earth version of NGL will have a similar hop in profile as what is expected to be seen on the Moon.

The hop can also be broken down by phase to see if there are any significant variations along the different steps of the trajectory. This data for the successful cases is presented in table 4.13. All deviations from the nominal Earth hop are around 1%. The differences from the lunar hop are under 3% for the traverse and descent. For the descent there is a 10% fuel increase from NGL, although the absolute magnitude of this is a fraction of a kilogram.

4.4.3.4 Remarks

The purpose of this section was to see how accurately an Earth version of the NGL vehicle could replicate what actual NGL will do in a lunar environment. The 3-DOF answer is that its successful cases, on average, closely resemble the lunar trajectory.

Although NGL and TALARIS are different vehicles, keep in mind that the latter is designed to be a testbed for lunar software. Thus, the control and guidance algorithms that run TALARIS will be the same which are implemented on NGL. For this reason it makes sense to compare the performances of the algorithms across the vehicles. In this section two main differences were highlighted. The first was the vehicle ascent and settling time, which was 3-seconds on TALARIS and is 7-seconds on NGL. The second is the number of failed cases: all were successful with EarthNGL, whereas TALARIS had an almost 2% failure rate. These observations suggest that the differences between the vehicles prevent the flight software, specifically a PID controller in HopperSim, from controlling them in the same manner [6]. For the actual TALARIS, this stresses the need for a software translator on the Earth vehicle that "tricks" the software into thinking it is running on a more advanced lunar hopper.

4.5   Conclusion

In order for TALARIS to be a successful prototype of the NGL lunar hopper, it must be able to emulate what is expected to be seen on the Moon. This chapter developed and used the HopperSim in order to run this analysis while introducing real-world dynamics such as pulsing thrusters, control loops, and errors and uncertainties on the actuators. The 3-DOF results show that due to the "failed hop" criteria, a TALARIS hop is successful 98% of the time. Within this, the hopper accurately follows what is projected to be seen on the Moon. It was also discovered that a level of EDF noise can be tolerated on the order of their required thrust output before the vehicle fails a majority of the time. Finally, the lunar NGL vehicle was compared to an Earth

---

[6]This is intuitive from a controls perspective, since by changing the vehicle the plant on which the controller acts is also being changed.

version with EDFs. The results were similar to that of TALARIS and LunarTALARIS, although there were some differences due to the performance of the software.

.

Chapter 5

Conclusion

5.1 Thesis Review

This thesis investigated the performance of planetary hoppers from three different angles. In Chapter 2, the Moon was used as the setting for a study of the ballistic and hover hops. The Hop Tradespace Tool was developed for this. From the results, it was determined that although the ballistic hop requires less fuel to achieve a given distance, the fuel penalty is an acceptable tradeoff for the ease of testing for a hover hop. This justified the use of the hover trajectory for the TALARIS and NGL vehicle hops.

Chapter 3 examines just how well TALARIS can execute a hover hop. The HTT was modified and used to evaluate the baseline TALARIS trajectory, and it was discovered that the baseline needed to be redesigned in order to stay within fuel constraints. After this was done, a trade study was performed to see how the baseline hop changed by varying certain parameters.

The ability of TALARIS to simply work is not enough; it must emulate what is expected to be seen on the Moon. Chapter 4 outlines the development of the HopperSim simulation tool and uses it to compare more realistic models of TALARIS and a lunar version. It also introduces uncertainty in the system. After compiling Monte Carlo runs, it was concluded that TALARIS does succeed in simulating the results of a lunar hop. Side-studies showed the effects of increased noise on the system

and compared the performance of NGL to an Earth version.

5.2   Limitations

The major limitation of this work is that the analysis took place in only the three translational degrees of freedom; rotations were not considered. This means that the asymmetries in actuator thrust, and thus torques, were not factored in to any of the results. The comparison between the ballistic and hover hops may look different if the fixed-attitude constraint is lifted. Also, although HopperSim showed that TALARIS is an accurate emulator of lunar hopper in 3-DOF, it is unknown to what extent the effects introduced by rotation will hinder performance or affect its tolerance for actuator noise.

Another limitation is that dispersions due to navigation errors were not included. Although the details of navigation systems were not a focus of this thesis, it is important to recognize that all of the results assume perfect sensors.

5.3   Future Work

There is much room for expansion upon the work included in this study. The following is a list of the possible next steps.

1. *Develop a 6-DOF Sim.* HopperSim has the capability to be upgraded to include three degrees of rotational freedom, and this would be necessary to do in order to capture the dynamics introduced by various torques. These can be both torques introduced by the actuators and those caused by the vehicle's center of mass shifting as fuel depletes.

2. *Develop an improved motor model.* The motor used in HopperSim is a simple lag developed experimentally. However, there is the possibility that there are unmodeled dynamics in the actual hardware which will cause problems with controlling the EDFs if left undiscovered. An in-depth study on the EDF motors would result in a more accurate model.

3. *Obtain more accurate error values.* The errors chosen in HopperSim were based on experimental data, but a separate experiment with actuator error would aid in getting these values more exact.

4. *Include sensors.* Introducing sensor error would bring another level of realism into the HopperSim.

5. *Implement the actual hopper guidance and control algorithms.* TALARIS will use the lunar hopper software to perform its hop. HopperSim could serve as a prototype to the hardware if these algorithms could be added within it.

6. *Try other planets.* With all of the above accomplished, HopperSim, and even the HTT, do not have to be restricted to the Moon. The thrust output of the EDF could be modifed to generate a gravity field of an asteroid or Mars. This will turn the Sim into a highly versatile tool for evaluating planetary hops.

THIS PAGE INTENTIONALLY LEFT BLANK

Appendix A

Additional modeling data

This appendix contains brief descriptions of the experiments run independently of this thesis which supplied data for the various simulations.

A.1   Motor Modeling

The EDFs in HopperSim are represented by the transfer function:

$$\frac{1}{(0.62 + 0.119)s + 1}$$

The time constant comes from the experimentally verified delays within the system. The controller gains were selected to be the following [1] :

- P = 0.0075

- I = 0.1124

- D = 0

---

[1]Courtesy of Mike Johnson (Draper) and Chris Han (MIT).

A.2 Actuator Uncertainty

The values for the EDF thrust standard devation was derived from the data in figure A-1. Figure A-1(top) shows the average results of an RPM ramp-up test with its standard deviations, and figure A-1(bottom) shows the corresponding average thrust. Together, they create an approximate thrust-to-RPM mapping [2]. The standard deviation at the highest RPMs (close to hover RPM) was found and converted to a thrust for use in HopperSim. A potential bias was approximated.

For the cold gas system, the noise values came from data related to the opening and closing times of the jets [3].

---

[2] Courtesy of Babak Cohanim (Draper).
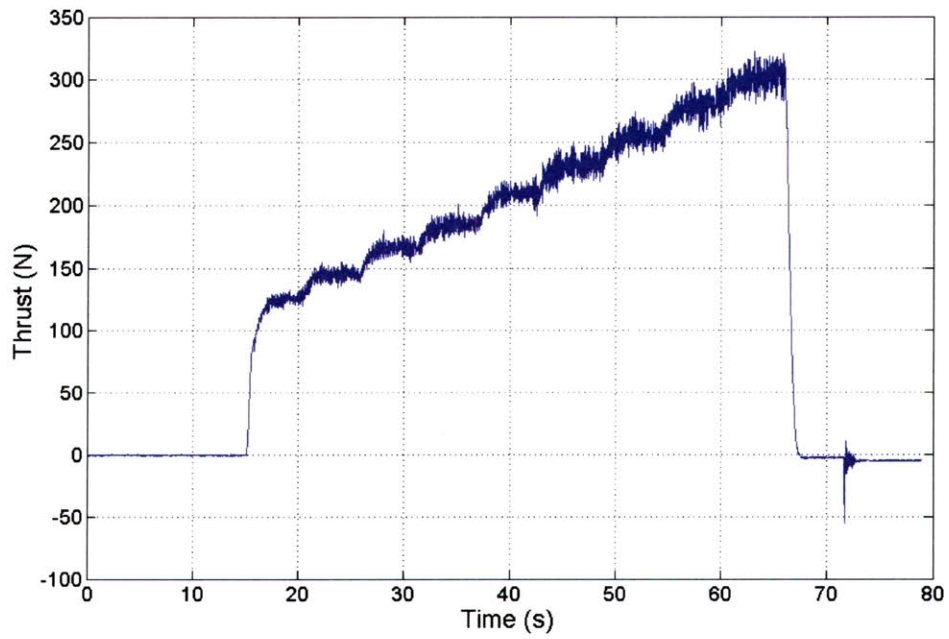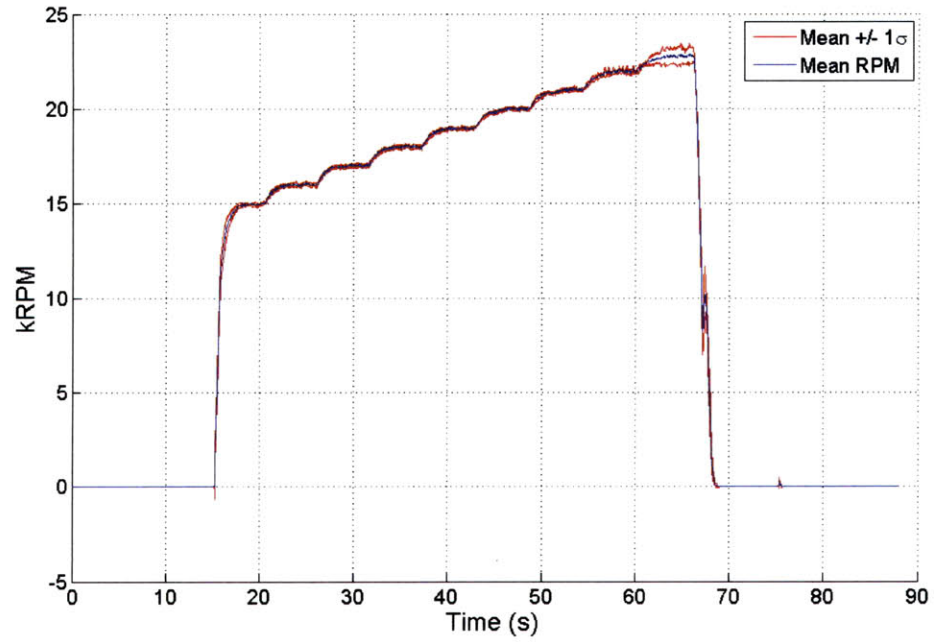[3] Courtesy of Zach Bailey (MIT) and Sarah Nothnagel (MIT).

Figure A-1: Results of EDF RPM ramp-up test (top) and corresponding thrust (bottom)

THIS PAGE INTENTIONALLY LEFT BLANK

Bibliography

[1] Jpl mars pathfinder homepage. `http://mars.jpl.nasa.gov/MPF/`, February 1997.

[2] Next giant leap homepage. `http://www.nextgiantleap.com/`, February 2009.

[3] Northrop grumman lunar lander x prize challenge homepage. `http://space.xprize.org/lunar-lander-challenge`, February 2009.

[4] Nasa mars pathfinder homepage. `http://www.nasa.gov/mission_pages/mars-pathfinder/`, February 2010.

[5] S. Alexander. Nasa and x prize announce winners of lunar lander challenge. `http://www.nasa.gov/home/hqnews/2009/nov/HQ_09-258-Lunar_Lander.html`, February 2009.

[6] A. Chaikin. The other moon landings. *Smithsonian Air and Space Magazine*, 2004.

[7] M.L. Hendry, K. Rojdev, J. Cheng, O. Faghfoor, A. Garcia, P. Giuliani, L. Hoag, C. Raskin, M. Rudolph, and O. Rahman. Leapfrog: Lunar entry and approach platform for research on ground. In *AIAA 2007 Conference and Exhibit*, 2007.

[8] Mars Institute. Mars exploration rovers - quick facts. `http://www.marsinstitute.info/epo/merfacts.html/`, February 2009.

[9] A. Ivankov. Luna 17/lunokhod 1. `http://nssdc.gsfc.nasa.gov/nmc/masterCatalog.do?sc=1970-095A`, February 2010.

[10] A. Ivankov. Luna 21/lunokhod 2. `http://nssdc.gsfc.nasa.gov/nmc/masterCatalog.do?sc=1973-001A`, February 2010.

[11] S. Kassel. Lunokhod-1 soviet lunar surface vehicle. Technical report, Advanced Research Projects Agency, 1971.

[12] M.W. Maimone, P.C. Leger, and J.J. Biesiadecki. Overview of the mars exploration rovers' autonomous mobility and vision capabilities. Technical report, Jet Propulsion Laboratory, California Institute of Technology, Pasadena, CA.

[13] NASA. Mars exploration rover mission homepage. `http://marsrovers.jpl.nasa.gov/home/index.html`, February 2010.